Hematopoietic stem cell–engrafted NOD/SCID/IL2Rγ^{null} mice develop human lymphoid systems and induce long-lasting HIV-1 infection with specific humoral immune responses

Satoru Watanabe,[1] Kazuo Terashima,[2] Shinrai Ohta,[3] Shigeo Horibata,[3] Misako Yajima,[4] Yoko Shiozawa,[1] M. Zahidunnabi Dewan,[2,3] Zhong Yu,[2] Mamoru Ito,[5] Tomohiro Morio,[6] Norio Shimizu,[1] Mitsuo Honda,[3] and Naoki Yamamoto[2,3]

[1]Department of Virology, Division of Medical Science, Medical Research Institute, Tokyo Medical and Dental University, Japan; [2]Department of Molecular Virology, Graduate School of Medicine, Tokyo Medical and Dental University, Japan; [3]AIDS Research Center, National Institute of Infectious Diseases, Tokyo, Japan; [4]Department of Infectious Diseases, National Research Institute for Child Health and Development, Tokyo, Japan; [5]Central Institute for Experimental Animals, Kanagawa, Japan; and [6]Department of Pediatrics and Developmental Biology, Graduate School of Medicine, Tokyo Medical and Dental University, Japan

Critical to the development of an effective HIV/AIDS model is the production of an animal model that reproduces long-lasting active replication of HIV-1 followed by elicitation of virus-specific immune responses. In this study, we constructed humanized nonobese diabetic/severe combined immunodeficiency (NOD/SCID)/interleukin-2 receptor γ-chain knockout (IL2Rγ^{null}) (hNOG) mice by transplanting human cord blood–derived hematopoietic stem cells that eventually developed into human B cells, T cells, and other monocytes/macrophages and dendritic cells associated with the generation of lymphoid follicle–like structures in lymphoid tissues. Expressions of CXCR4 and CCR5 antigens were recognized on CD4$^+$ cells in peripheral blood, the spleen, and bone marrow, while CCR5 was not detected on thymic CD4$^+$ T cells. The hNOG mice showed marked, long-lasting viremia after infection with both CCR5- and CXCR4-tropic HIV-1 isolates for more than the 40 days examined, with R5 virus–infected animals showing high levels of HIV-DNA copies in the spleen and bone marrow, and X4 virus–infected animals showing high levels of HIV-DNA copies in the thymus and spleen. Furthermore, we detected both anti–HIV-1 Env gp120– and Gag p24–specific antibodies in animals showing a high rate of viral infection. Thus, the hNOG mice mirror human systemic HIV infection by developing specific antibodies, suggesting that they may have potential as an HIV/AIDS animal model for the study of HIV pathogenesis and immune responses. (Blood. 2007; 109:212-218)

Introduction

Current animal models for either human immunodeficiency virus type 1 (HIV-1) or simian immunodeficiency virus (SIV) suffer from the lack of a system precisely mirroring human HIV infection and the progression to disease state.[1] In current animal models with HIV infection, such as chimpanzees, animals do not develop AIDS.[1] Past animal models for HIV infection have relied on humanized severe combined immunodeficiency (hSCID) mice models to study prospective anti-HIV drugs and vaccines. SCID-hu (Thy/Liv) mice, engrafted with human fetal thymus and liver tissue in the renal subcapsular region, were first reported as the small-animal model.[2] Because human T cells are generated within the engrafted thymus, this model has been used for the study of thymopoiesis[3-6] and hematopoiesis[7,8] under the burden of HIV-1 infection. However, this model allows for a limited systemic HIV-1 infection, which is restricted mainly to the engrafted thymus. Another HIV mouse model, hu-PBL–SCID mice engrafted with human peripheral blood mononuclear cells (PBMCs),[9] has been actively used as a tool in developing antiretroviral therapy.[9-11] However, the infection persists for only a short time in association with rapid loss of CD4$^+$ T cells because there is no active hematopoiesis or thymopoiesis.[9,12,13] Furthermore, these mouse models fail to mirror certain key aspects of the human immune response, lacking normal lymphoid tissue and functional human antigen-presenting cells such as dendritic cells (DCs).[14] Thus, although these mouse models are valuable as animal models for HIV infection, the development of a mouse model more analogous to human HIV infection is needed if we are to better understand HIV pathogenesis and develop successful anti-HIV therapies and preventive vaccines.

To solve the difficult issue about the development of an ideal HIV mouse model, we initially selected a humanized nonobese diabetic (NOD)/SCID interleukin-2 receptor (IL-2R) γ-chain knockout (NOG) mouse[15] as a model animal because it has been suggested that multilineage cells, including human T, B, and natural killer (NK) cells, differentiate in these mice when given transplants of human CD34$^+$ hematopoietic stem cells.[16-18] In the current study, we further reveal the kinetics of differentiation of human B and T cells, monocytes/macrophages, and DCs in the mice that received transplants, and we characterize the animals by infection with both CCR5 (R5)– and CXCR4 (X4)-tropic HIV strains. Since our hNOG mice show stable and systemic infection of both R5- and X4-tropic HIV for more than

Submitted April 20, 2006; accepted August 12, 2006. Prepublished online as *Blood* First Edition Paper, September 5, 2006; DOI 10.1182/blood-2006-04-017681.

The publication costs of this article were defrayed in part by page charge payment. Therefore, and solely to indicate this fact, this article is hereby marked "advertisement" in accordance with 18 USC section 1734.

the 40 days studied, and HIV-specific antibodies are detectable in the animals with high plasma viral loads and HIV-DNA copy numbers, we also discuss the suitability of HIV-hNOG mice as an animal model for HIV-1 infection.

Materials and methods

Transplantation of human CB-derived hematopoietic stem cells in NOG mice

Human cord blood (CB) was obtained from Saiseikai Central hospital (Minato-ku, Tokyo, Japan) and Tokyo Cord Blood Bank (Katsushika-ku, Tokyo, Japan) after obtaining informed consent. All research on human subjects was approved by the Institutional Review Board of each institution participating in the project. CB mononuclear cells were separated by Ficoll-Hypaque density gradient. $CD34^+$ hematopoietic stem cells were isolated using a magnetic-activated cell sorting (MACS) Direct CD34 Progenitor Cell Isolation Kit (Miltenyi Biotec, Bergisch Gladbach, Germany) according to the manufacturer's instructions. More than 95% of $CD34^+$ cells were positively selected after 2 time-enrichment manipulations. Cells were either immediately used for the transplantation or frozen until use. NOG mice were obtained from the Central Institute for Experimental Animals (Kawasaki, Japan) and maintained under specific pathogen–free (SPF) conditions in the animal facility of the National Institute of Infectious Diseases (NIID; Tokyo, Japan). Mice used in these studies were free of known pathogenic viruses, herpes viruses, bacteria, and parasites. They were housed in accordance with the Guidelines for Animal Experimentation of the Japanese Association for Laboratory Animal Science (1987) under the Japanese Law Concerning the Protection and Management of Animals, and were maintained in accordance with the guidelines set forth by the Institutional Animal Care and Use Committee of NIID, Japan. Once approved by the Institutional Committee for Biosafety Level 3 experiments, these studies were conducted at the Animal Center, NIID, Japan, in accordance with the requirements specifically stated in the laboratory biosafety manual of the World Health Organization. Female mice (6 to 10 weeks old) were irradiated (300 cGy) and 1×10^4 to 1.2×10^5 $CD34^+$ cells were intravenously injected within 12 hours.

Flow cytometry

The purity of CB-derived $CD34^+$ cells after separation was evaluated by double staining with FITC-conjugated anti–human CD45 (J.33) and PE-conjugated anti–human CD34 (Class III 581) (all from Beckman Coulter, Fullerton, CA). After transplantation (1-7 months), peripheral blood, spleens, bone marrow (BM), and thymi were collected for flow cytometric analysis following staining with the following monoclonal antibodies (mAbs): FITC-conjugated anti–human CD45 (J.33), CD3 (UCHT1), CD4 (13B8.2), CD19 (J4.119), CD45RO (UCHL1) (all from Beckman Coulter), and CCR5 (2D7; BD Pharmingen, San Diego, CA); PE-conjugated anti–human CD4 (13B8.2), CD8 (B9.11), CD19 (J4.119), CD45RA (ALB11) (all from Beckman Coulter), and CXCR4 (44717; R&D Systems, Minneapolis, MN); anti–mouse CD45 (YW62.3; Beckman Coulter); ECD-conjugated anti–human CD45 (J.33; Beckman Coulter); and PC5-conjugated anti–human CD8 (T8) and CD14 (Rm052) (all from Beckman Coulter). Flow cytometric analysis was conducted by 2- or 4-color staining using an EpicsXL (Beckman Coulter).

Immunohistochemistry

Organs were snap-frozen following embedding in OCT compound (Sakura Finetechnical, Tokyo, Japan). Frozen sections were air-dried and fixed in acetone. HIV-1–infected organs were fixed in 4% paraformaldehyde and embedded in OCT compound following immersion in gradient sucrose (5%-30%). Fixed samples were stained with the following mAbs: anti–human CD45 (1.22/4014; Nichirei, Tokyo, Japan), CD3 (UCHT1; DAKO, Glostrup, Denmark), CD20 (L26; DAKO), CD68 (KP1; DAKO), CD205 (MG38; eBioscience, San Diego, CA), and DRC-1 (R4/23; DAKO) for follicular dendritic cells (FDCs); anti–mouse FDC-M1 (BD Pharmingen) for murine FDCs; and HIV-1 Gag p24 (DAKO) for detection of infected cells. Biotin-labeled goat $F(ab')_2$ anti–mouse immunoglobulin (Ig; ICN Biomedicals, Aurora, OH)– or biotin-labeled mouse $F(ab')_2$ anti–rat IgG (Jackson ImmunoResearch Laboratories, West Grove, PA) was used as the secondary antibody. Samples were treated with alkaline phosphatase (AP) or horseradish peroxidase (HRP)–streptavidin conjugate (ZYMED Laboratories Inc, San Francisco, CA). BCIP/NBT, DAB, or AEC (all from DAKO) was used for the visualization. Photographs were taken by light microscopy (Leica DMRA; Leica Microsystems Wetzlar, Wetzlar, Germany) using Leica HC PLAN APO lenses (10×/0.40 NA PH1). Leica Q550 was used for image processing.

Measurement of human Igs in mice plasma

Plasma concentrations of human IgM, IgG, and IgA in NOG mice that received transplants of human stem cells were determined by conventional human Ig quantitation assay at BML Inc (Tokyo, Japan).

Cells and viruses

Human embryonic kidney 293T cells and monkey kidney COS7 cells were cultured in RPMI 1640 supplemented with 10% fetal bovine serum (FBS) and antibiotics. The 293T cells and COS7 cells were used for transfection of DNA plasmids containing HIV-1_{JRCSF} and simian/human immunodeficiency virus (SHIV)–C2/1, respectively. The SHIV-C2/1 strain contains the *env* gene of pathogenic HIV-1 strain 89.6.[19] Cell-free supernatant was collected and stored at −80°C before use. A primary clinical isolate, HIV-1_{MNp}, was kindly provided by Dr J. Sullivan of the University of Massachusetts Medical School (Worcester, MA). PBMCs isolated from HIV-1–seronegative individuals were cultured in RPMI 1640 supplemented with 10% FBS and antibiotics with 5 μg of phytohemagglutinin (PHA)/mL for 3 or 7 days (PHA-PBMCs). HIV-1_{MNp} was propagated in PHA-PBMCs, and cell-free virus stocks were stored at −80°C.

The 50% tissue-culture infectious dose ($TCID_{50}$) was determined using PHA-PBMCs and the endpoint dilution method. A 4-fold series of dilution was prepared from the virus stock, and then cells were mixed and cultured for 7 days for X4–HIV-1 and 14 days for R5–HIV-1 in RPMI 1640 supplemented with 20% FBS and antibiotics. The endpoints were determined by screening for the p24 antigen using Lumipulse (Fujirevio, Tokyo, Japan).

HIV-1 infection

All procedures for the infection and maintenance of NOG mice were performed in Biosafety Level 3 facilities at NIID under standard caging conditions. On days 102 to 132 after stem cell transplantation, 16 mice were inoculated intravenously with R5-tropic HIV-1_{JRCSF} (65 000 $TCID_{50}$) or X4-tropic SHIV-C2/1 (50 000 $TCID_{50}$). On days 18 to 43 after inoculation, plasma was collected to determine HIV-RNA copy numbers, and spleen cells were prepared as single-cell suspensions to analyze the CD4/CD8 ratio using flow cytometry. A number (14) of other mice were inoculated intravenously with R5-tropic HIV-1_{JRCSF} (200 or 65 000 $TCID_{50}$) or X4-tropic HIV-1_{MNp} (180 or 20 000 $TCID_{50}$) on days 126 to 146 after transplantation. On days 18 to 40 after inoculation, plasma was collected for the determination of HIV-RNA copy numbers, and single-cell suspensions of the spleen, BM, and thymus were prepared for HIV-DNA measurement. The CD4/CD8 ratio in the spleen and percentages of human $CD45^+$ cells in organs were analyzed using flow cytometry.

Virologic analysis

Plasma viral RNA copy numbers were measured using a real-time quantification assay based on the TaqMan system (Applied Biosystems, Foster City, CA). Plasma viral RNA was extracted and purified using a QIAamp Viral RNA Mini Kit (Qiagen, Valencia, CA). The RNA was subjected to reverse transcription (RT) and amplification using a TaqMan One-Step RT–polymerase chain reaction (PCR) Master Mix Reagents Kit (PE Biosystems, Foster City, CA) with HIV-1 gag consensus primers

(forward, 5′-GGACATCAAGCAGCCATGCAA-3′; and reverse, 5′-TGCTATGTCACTTCCCCTTGG-3′) and an HIV-1 gag consensus TaqMan probe (FAM-5′-ACCATCAATGAGGAAGCTGCAGAA-3′-TAMRA). For SHIV-C2/1 analysis, primers (forward, 5′-AATGCAGAGCCCCAAGAAGAC-3′; and reverse, 5′-GGACCAAGGCCTAAAAAACCC-3′) and a TaqMan probe (FAM-5′-ACCATGTTATGGCCAAATGCCCAGAC-3′-TAMRA) were designed for targeting the SIVmac239 gag region.[20] Probed products were quantitatively monitored by their fluorescence intensity with the ABI7300 Real-Time PCR system (PE Biosystems). To obtain control RNA for quantification, HIV-1 gag RNA and SIVmac239 gag RNA were synthesized using T7 RNA polymerase and pKS460. Viral DNA was extracted and purified using a QIAamp DNA Mini Kit (Qiagen). Determination of HIV-1 DNA copy numbers was performed by real-time PCR assay with TaqMan Master mixture (PE Biosystems). Primers (forward, 5′-GGCTAACTAGGGAACCCACTG-3′; and reverse, 5′-CTGCTAGAGATTTTCCACACT-3′) and probes (FAM-5′-TAGTGTGTGCCCGTCTGTTGTGTGAC-3′-TAMRA) were designed for targeting the HIV-1 long terminal repeat region, R/U5. The viral DNA was quantified using LightCycler (Roche Diagnostics, Almere, The Netherlands). Viral RNA and DNA were calculated based on the standard curve of control RNA and DNA. All assays were carried out in duplicate.

HIV-antigen ELISA

Levels of anti–HIV-1 Igs against recombinant HIV-1_{IIIB} Env gp120, recombinant HIV-1_{MN} Env gp120, and recombinant HIV-1_{IIIB} Gag p24 (all from ImmunoDiagnostics Inc, Woburn, MA) in plasma from HIV-1–infected and –uninfected control mice were determined using a standard enzyme-linked immunosorbent assay (ELISA). Microplates (96-well) were coated overnight with 200 ng/well antigens, and plasma diluted 1:20, 1:60, and 1:180 with PBS were incubated for 1 hour. AP-labeled anti–human Igs (γ, α, and μ; Sigma-Aldrich, St Louis, MO) were used as secondary antibodies. P-nitrophenylphosphate (pNPP) Solution (WAKO Chemical USA, Richmond, VA) was used for the visualization. The enzyme reaction was stopped by addition of 0.1 M NaOH and read at 405 nm. All assays were carried out in triplicate.

Statistical analysis

Data were expressed as the mean value ± standard deviation (SD). Significant differences between data groups were determined by 2-sample Student *t* test analysis. A *P* value less than .05 was considered significant.

Results

Reconstitution of human lymphoid systems in hNOG mice

The initial studies describing the construction of humanized SCID mice used the human PBMC for infection of immunodeficiency viruses.[9,12,21] However, these hu-PBL-SCID mice showed a partial infection to the R5 virus and a relatively limited period of viral replication. To construct a more suitable mouse model mimicking HIV-1 infection in humans, we selected human CB stem cells as a transplant for NOG mice. NOG mice were inoculated intravenously with human CD34$^+$ hematopoietic stem cells, and their development of human lymphoid systems were then monitored. After transplantation (2 months), human CD45$^+$ leukocytes were recognized in both PB and the spleen, but most of the cells were human B cells (Figure 1A). Human T cells began to be recognized clearly in PB and the spleen 4 months after transplantation (Figure 1B) and gradually increased in level, as did human B cells (Figure 1C).

In Figure 1D, we summarized percentages of human CD3$^+$ T cells in human CD45$^+$ cells from 38 mice from 39 to 213 days after transplantation. Human CD3$^+$ T cells clearly increased 100 days after transplantation in both PB and the spleen. After transplantation (4 months), human CD3$^+$ T cells in the spleen preferably expressed CD45RA rather than CD45RO (70.8% ± 13.4% and 27.3% ± 38.8% in CD3$^+$ T cells, respectively; n = 5; Figure 1E), demonstrating that most of the T cells were in a naive state. In addition, plasma taken from 5 mice 113 to 143 days after transplantation showed that all mice produced human IgM, with concentrations ranging from 0.025 to 0.5 g/L, and that human IgG and IgA was also detected in some of the mice (ranges, 0.015-0.18 g/L and 0.003-0.012 g/L, respectively) (data not shown).

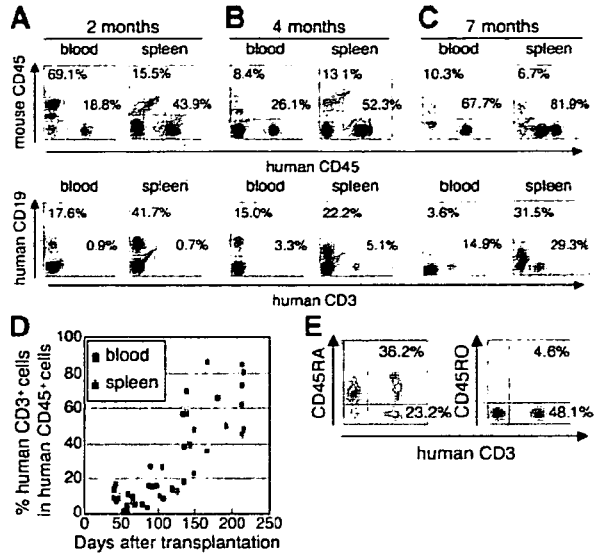

Figure 1. Flow cytometric analysis of human T cells in the peripheral blood and spleen in NOG mice given intravenous transplants of human CB-derived CD34$^+$ cells. (A-C) Representative profiles of the mice 2 months (A), 4 months (B), and 7 months (C) after transplantation. The ratio of human to murine CD45$^+$ cells and that of human CD3$^+$ to CD19$^+$ cells show an incremental increase in human CD45$^+$ cells and human CD3$^+$ cells from 2 to 7 months. (D) Change of net percentages of human CD3$^+$ T cells among human CD45$^+$ cells in peripheral blood and the spleen from 38 mice 39 to 213 days after transplantation. (E) CD45RA is more efficiently expressed than CD45RO on human CD3$^+$ T cells in spleen. A gate was set on the human CD45$^+$ population. The fluorescence-activated cell sorting (FACS) profile is representative of 1 in a group of 5 mice.

By 7 months after transplantation, human CD45$^+$ leukocytes comprised more than 80% to 90% of mononuclear cells in the spleen (Figure 1C), and most of the mice showed symptoms of a wasting condition and a hunched back. Based upon these results, we determined that the suitable period for HIV inoculation would be 4 to 5 months after transplantation.

Formation of lymphoid structures, including monocytes/macrophages, DCs, and FDCs

Next, using the hNOG mice at 4 months after transplantation, we investigated lymphoid structure formation and the development of human monocytes, macrophages, DCs, and FDCs, which are very important factors not only for elicitation of immune responses against foreign antigens, but also for the spread of HIV-1 infection in a body.[22-24] Human CD14$^+$ monocytes were detected in PB, the spleen, and BM using flow cytometry (Figure 2A). During immunohistochemical analysis, human CD45$^+$ leukocytes gathered in a form of follicle-like structures (FLSs) at the end of the central artery in the spleen (Figure 2B). From a serial section of the same region (Figure 2B-G), these structures consisted mainly of human CD20$^+$ B cells (Figure 2C) admixed with a small number of human CD3$^+$ T cells (Figure 2D). Hardly any human FDCs positive for DRC-1 were detected (data not shown), whereas a

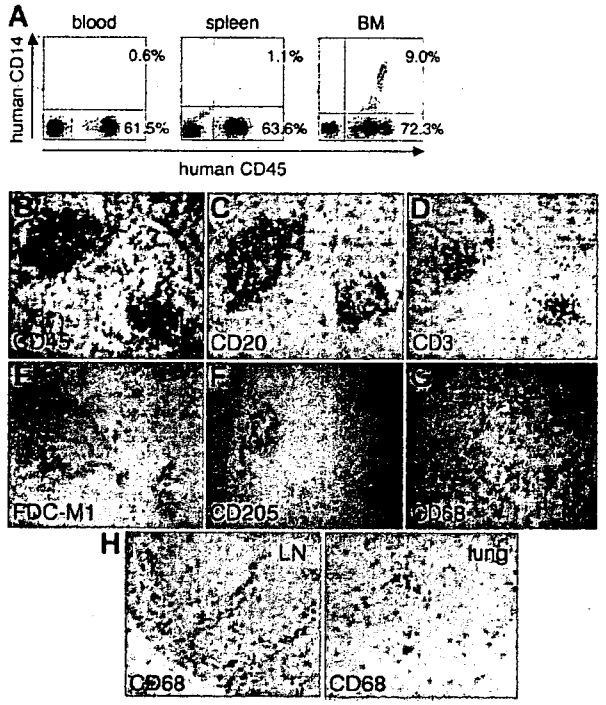

Figure 2. Flow cytometric analysis and immunohistochemical analysis of the expression of myelomonocytic markers in hNOG mice 4 months after transplantation. (A) Human CD14$^+$ monocytes/macrophages are recognized in peripheral blood, the spleen, and BM. (B-G) Immunohistochemical findings from serially sectioned spleen for the expressions of human CD45 (B), human CD20 (C), human CD3 (D), murine FDC (E), human CD205 (F), and human CD68 (G). (H) Human CD68$^+$ macrophages are also detected in the medulla of the LN and lung. Visualization was performed with BCIP (B-D, F-G), DAB (E), and AEC (H). Original magnification, ×100.

loose network of murine FDCs positive for FDC-M1 was recognized in the distal portion of the FLSs (Figure 2E). Human CD205$^+$ DCs were predominantly detected in a cluster form within the FLSs (Figure 2F), while human CD68$^+$ macrophages were scattered throughout the spleen (Figure 2G). Many human CD68$^+$ macrophages were also observed in various other organs, including the lymph nodes (LNs) and the lungs (Figure 2H).

Expression of HIV-1 coreceptors on CD4$^+$ cells in various tissues

Since the development of lymphoid tissues was recognized in hNOG mice, we focused on the expressions of HIV-1 coreceptors CXCR4 and CCR5 on human CD4$^+$ cells in these tissues. CXCR4 antigen was expressed in 36.5% ± 4.2% (n = 4) of the CD4$^+$ cells in PB (Figure 3A) and 78.1% ± 17.1% (n = 5) in the spleen (Figure 3B). CCR5$^+$ cells were detected in 15.5% ± 1.8% (n = 4) of CD4$^+$ cells in PB and 28.6% ± 12.6% (n = 5) in the spleen (Figure 3A-B). In the thymus, CD4$^+$CD8$^+$ thymocytes existed in 82.9% ± 4.4% (n = 5) as well as small numbers of CD4$^+$CD8$^-$ cells (6.4% ± 2.4%; n = 5) and CD4$^-$CD8$^+$ cells (7.7% ± 3.0%; n = 5), with the CXCR4 antigen expressed in 50.1% ± 4.5% (n = 5) of CD4$^+$ cells, while, as with normal human thymocytes,[25] CCR5$^+$ cells were almost undetectable, with less than 1% (0.6% ± 0.1%; n = 5) (Figure 3C). Human CD3$^+$ T cells and CD14$^+$ monocytes in BM were detected only in 3.2% ± 2.1% and 5.8% ± 3.8%, respectively, while CD4$^+$ cells were recognized in 18.1% ± 6.5%, with many expressing both CXCR4 (75.0% ± 23.1%) and CCR5 (81.3% ± 6.6%; n = 5; Figure 3D). Thus, distributions of HIV-1 coreceptor–positive cells in these lymphoid tissues suggest that the hNOG mice allow for sufficient development of human cells to make the study of HIV-1 pathogenesis possible.

Both R5- and X4-tropic HIVs efficiently infect and replicate in hNOG mice

In our preliminary study, using low and high doses of challenge virus, no viral infection was detected in any of the virus-inoculated hNOG mice at 7 days after infection, while some showed detectable plasma viral loads at 14 days (data not shown). Then, we prepared 16 hNOG mice that received transplants of stem cells and inoculated them with a high dose of R5-tropic HIV-1_{JRCSF} (65 000 $TCID_{50}$) and X4-tropic SHIV-C2/1 (50 000 $TCID_{50}$) intravenously through the tail vein at 102 to 132 days after transplantation. Upon HIV-1_{JRCSF} infection, viral copy numbers in plasma rose to a level of 1.6×10^5 to 5.8×10^5 copies/mL (n = 4) on day 33 and 2.0×10^5 to 4.7×10^5 copies/mL on day 43 (n = 4) (Figure 4A). Moreover, for SHIV-C2/1 infection, viral copy numbers in plasma were 1.6×10^3 to 3.2×10^5 copies/mL on day 18 (n = 4) and reached 5.4×10^4 to 1.1×10^5 copies/mL on day 42 (n = 4; Figure 4B). In these mice, no significant decline in the CD4/CD8 ratio was observed throughout entire period of follow-up for the R5-tropic virus infection, while CD4$^+$ cell decline was detected for the X4-tropic virus infection on day 42 after infection ($P = .044$) but not on day 18 after infection (Figure 4C). Four mice that did not receive transplants of human stem cells showed no detectable levels of plasma viral load (less than 500 copies/mL) following HIV/SHIV inoculation (data not shown).

To confirm HIV infection, we used immunohistochemistry to detect the presence of the p24 antigen of the HIV-1 Gag protein in various tissues of mice showing viremia. p24$^+$ cells were clearly identified in the spleen, LN, and lungs (Figure 4D), which include macrophage-like cells.

Different distributions of R5- and X4-tropic viruses in lymphoid tissues

A number of mice (14) were further analyzed for HIV-1 infection on days 126 to 146 after transplantation with a low dose (200 $TCID_{50}$) or a high dose (65 000 $TCID_{50}$) of R5-tropic HIV-1_{JRCSF} and a low dose (180 $TCID_{50}$) or a high dose (20 000 $TCID_{50}$) of X4-tropic HIV-1_{MNp}. Consequently, 2 of the 4 mice given a low

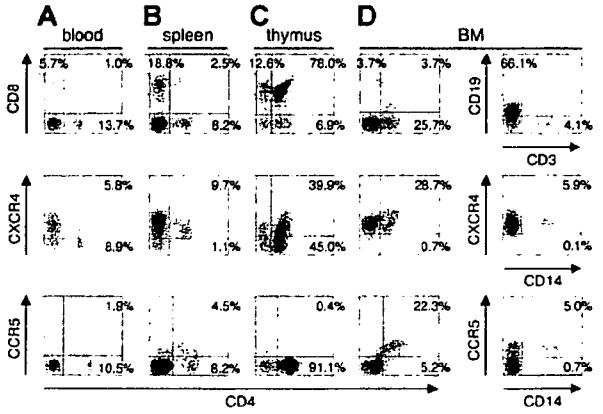

Figure 3. Surface expression of HIV-1 coreceptors on CD4$^+$ cells in various organs of mice 4 months after transplantation. A representative FACS profile of human CXCR4 and CCR5 on CD4$^+$ cells shows the existence of CXCR4$^+$CD4$^+$ and CCR5$^+$CD4$^+$ cells in blood (A), spleen (B), and BM (D), but no CCR5$^+$CD4$^+$ cells in the thymus (C). BM results show that many CD4$^+$ cells are neither CD3$^+$ T cells nor CD14$^+$ monocytes. A gate was set on the human CD45$^+$ population.

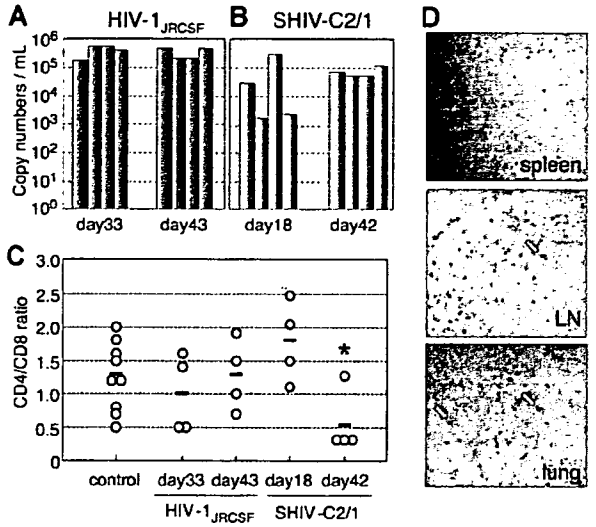

Figure 4. The numbers of RNA viral copies in plasma, CD4⁺/CD8⁺ T-cell ratios in the spleen, and p24 detection in the immunohistochemistry of HIV/SHIV-infected mice. (A) Viral copy numbers of 8 mice inoculated with a high infectious dose of HIV-1_{JRCSF} (65 000 $TCID_{50}$) and killed on days 33 and 43 after inoculation. (B) Viral copy numbers of 8 mice inoculated with a high infectious dose of SHIV-C2/1 (50 000 $TCID_{50}$) and killed on days 18 and 42 after inoculation. Note that all the mice showed high levels of viremia that lasted more than 40 days after inoculation. (C) CD4/CD8 cell ratios in the spleens of 16 infected mice and 9 uninfected control mice. Control mice were not inoculated with HIV/SHIV and were killed on days 105 to 166 after stem cell transplantation. There was no significant rapid loss of CD4⁺ cells in HIV-1_{JRCSF}–infected mice, while a decline of the CD4/CD8 ratio was detected in SHIV-C2/1–infected mice on day 42 after infection compared with uninfected control mice (*$P < .05$). The short bars indicate the means of each group. (D) P24⁺ cells are clearly observed in the spleen, LNs, and lungs. Arrow indicates p24 positive for macrophage-like cells. Original magnification, ×100.

dose of HIV-1_{JRCSF} and 2 of the 3 mice given a low dose of HIV-1_{MNp} were successfully infected (Table 1), suggesting that each dose represents an approximately 50% infectious dose of HIV for hNOG mice. High HIV-DNA copy numbers were mainly detected in the spleen and BM of the HIV-1_{JRCSF} –infected mice, and in the thymus and spleen of the HIV-1_{MNp}–infected mice, while their BM showed lower copy numbers (Table 1).

Generation of HIV-specific antibodies in hNOG mice at a high multiplicity of infection

We then tested for generation of human antibodies against HIV-1 from these 14 mice by HIV antigen-specific ELISA. The sera of mice no. 136-3 and no. 157-3 infected with HIV-1_{JRCSF} and HIV-1_{MNp}, respectively, showed significant levels of human antibodies specific for HIV-1_{IIIB}-Env gp120 (Figure 5A), HIV-1_{MN}-Env gp120 (Figure 5B), and HIV-1_{IIIB}-Gag p24 (Figure 5C). In addition, no. 157-4 sera from an HIV-1_{MNp}–infected animal was also weakly positive for their Env and Gag antigens. These animals showed intense plasma viral loads and enhanced proviral DNA copies in the spleen, BM, and thymus (Table 1), suggesting that hNOG mice inoculated with high doses of HIV and showing high rates of viral infection develop HIV-1–specific humoral immune responses that are analogous to those seen in human anti-HIV B-cell responses.

Discussion

Current small-animal models fall short of accurately mirroring human HIV-1 infection and thus have limited usefulness in analyzing the natural course of its progression to the disease state and in developing antiviral countermeasures. Although successful HIV-1 infections in immunodeficiency mice humanized with PBMCs have been reported,[12,13,21] transplanted human cells are soon depleted and do not elicit virus-specific immune responses, shedding little light on pathogenesis and vaccine development. By using NOG mice that received hematopoietic stem cell transplants showing high rates of viral infection, we demonstrated HIV-specific antibody responses and viral infection parameters, including the following: (1) similar levels of susceptibility to both R5- and X4-tropic HIV-1; (2) high levels of viremia stably observed over 40 days; (3) immunohistochemical detection of infected cells in various organs; and (4) a distinct tissue distribution for R5- versus X4-tropic HIV-1s.

Among CD4⁺ T cells, CXCR4 antigen is primarily expressed on naive and CCR5 on activated or memory cells.[26] hu-PBL-SCID mice become susceptible to R5-tropic HIV-1 strains,[27] since T cells

Table 1. Comparison of viral RNA copies in plasma and HIV-DNA copies in the spleen, BM, and thymus from hNOG mice receiving low- and high-dose viral inoculations

Mouse ID no.	HIV strain	$TCID_{50}$	Time after inoculation, d	RNA viral copies/mL	CD4/CD8 ratio	HIV-DNA copies/10^6 human cells		
						Spleen	BM	Thymus
Low-dose viral inoculation group								
113-1	HIV-1_{JRCSF}	200	18	6 240	1.8	34 177	11 785	3 495
112-2	HIV-1_{JRCSF}	200	18	<500	1.2	< 100	< 100	< 100
113-2	HIV-1_{JRCSF}	200	40	6 177	1.6	25 855	27 920	3 473
112-3	HIV-1_{JRCSF}	200	40	<500	0.9	< 100	< 100	<100
112-4	HIV-1_{MNp}	180	18	72 477	1.3	18 873	100	ND
113-4	HIV-1_{MNp}	180	40	70 667	0.3	4 947	653	32 163
112-1	HIV-1_{MNp}	180	40	<500	0.9	< 100	< 100	< 100
High-dose viral inoculation group								
136-3	HIV-1_{JRCSF}	65 000	25	252 381	0.8	958 871	1 797 600	232 155
136-2	HIV-1_{JRCSF}	65 000	29	50 167	0.7	41 172	54 521	8 600
141-1	HIV-1_{JRCSF}	65 000	30	67 667	2.2	27 735	52 430	429
161-3	HIV-1_{JRCSF}	65 000	30	13 847	0.9	104 466	14 653	111 080
157-3	HIV-1_{MNp}	20 000	31	1 253 925	0.5	41 053	56 802	976 556
157-4	HIV-1_{MNp}	20 000	31	147 973	0.6	3 634	262	40 796
161-6	HIV-1_{MNp}	20 000	31	108 073	1.7	4 991	< 100	3 673

Seven mice inoculated with a low infectious dose of HIV-1_{JRCSF} (200 $TCID_{50}$) or HIV-1_{MNp} (180 $TCID_{50}$), and 7 mice receiving a high infectious dose of HIV-1_{JRCSF} (65 000 $TCID_{50}$) or HIV-1_{MNp} (20 000 $TCID_{50}$) were listed.

ND indicates not done.

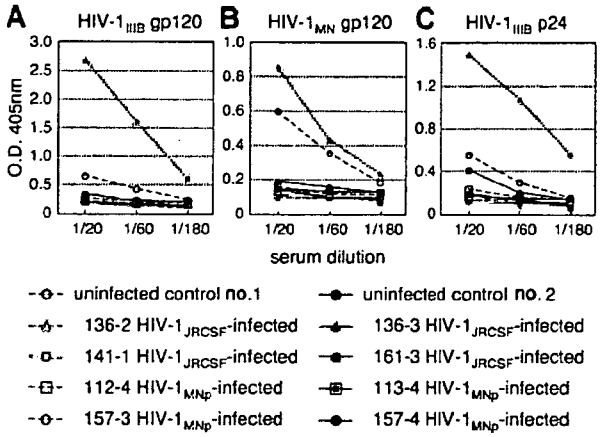

Figure 5. Detection of anti–HIV-1 antibodies from the plasma of HIV-1–infected mice. An ELISA assay was conducted by using plasma from 14 mice inoculated with either HIV-1_{JRCSF} or HIV-1_{MNp}, and from 2 uninfected control mice. Representatives (n = 8) of the 14 HIV-1–inoculated mice, and the 2 uninfected mice, are shown in the panels. Measurements of specific human antibodies for HIV-1_{IIIB} gp120 (A), HIV-1_{MN} gp120 (B), and HIV-1_{IIIB} p24 antigens (C) were shown. Results are expressed as the means from triplicate assays in 3 different experiments.

are initially activated in the xenogenic environment and then become anergic.[14] In contrast, SCID-hu (Thy/Liv) mice are more susceptible to X4 than to R5 strains[6] because HIV-1 infection is restricted mainly to the engrafted thymus that is primarily comprised of immature T cells, suggesting that this model may not be practical overt HIV infection. Our study represents the first attempt to infect NOG mice that received transplants of human hematopoietic stem cells with HIV-1. Very similar infection rates were seen for both R5 and X4 strains in the mouse model. Flow cytometry revealed both $CXCR4^+CD4^+$ and $CCR5^+CD4^+$ cells in PB, the spleen, and BM, but only CXCR4 on thymic $CD4^+$ T cells. It also showed the scattering of human macrophages, known to be susceptible to R5-tropic HIV-1 strains[28,29] and the source of HIV-1,[23,30-32] throughout various organs. $p24^+$ macrophage-like cells were detected in these organs after R5-tropic HIV-1_{JRCSF} infection. These data may help explain the susceptibility of hNOG mice to both R5- and X4-tropic HIV strains and also shed light on the active replenishment of these target cells in mice.

SCID mouse systems have been actively used in the evaluation of anti–HIV-1 drugs.[9,11,21] In most cases, HIV-1 detection levels reach a peak within a month after inoculation and level off, accompanied by $CD4^+$ T-cell depletion.[3,12,13] Although suitable for short-term experiments, it is also true that these models require large numbers of mice because of large variations in infection efficiency. In contrast, very stable infections were noted in our hNOG mice that were inoculated with a high dose of HIVs. They did not show rapid CD4/CD8 decrease in spite of high levels of viremia persisting for more than 40 days. Efficient hematopoiesis and thymopoiesis of human cells probably compensated for the loss of $CD4^+$ T cells, allowing for persistent infection. This capacity of the hNOG mouse system makes it attractive as a model for the long-term evaluation of anti–HIV-1 drugs. In addition to destroying mature blood cells, altered hematopoiesis in BM and the thymus has also been reported to be responsible for immunodeficiency in patients with AIDS.[33,34] To study hematopoietic abnormalities in HIV-1 infection, both SCID-hu (Thy/Liv) mice[8,35,36] and SIV- or SHIV-infected macaque models[20,37-39] have been used. The current hNOG mouse system, in which human cells are efficiently reproduced from stem cells and then settled into hematopoietic organs, offers a promising model for the study of events that occur after infection not only with R5-tropic HIV-1 but also with X4-tropic HIV-1. Indeed, the BM of hNOG mice infected with R5-tropic HIV-1 exhibited exceptionally elevated levels of HIV-DNA copies. On the other hand, the thymus of X4-tropic HIV-1_{MNp}–infected hNOG mice yielded large numbers of HIV-DNA copies, which seemed to correlate with the predominant expression of CXCR4 on the thymocytes. Thus, further observation is essential to address whether AIDS symptoms such as considerable $CD4^+$ T-cell depletion and hematopoietic abnormalities eventually occur in these mice.

It is noteworthy that human antibodies against both HIV-1 Env gp120 and Gag p24 antigens were detected in mice no. 136-3, no. 157-3, and no. 157-4 after exposure to high titers of HIV-1, suggesting that hNOG mice have the ability to respond to HIV-1 antigens. This encourages us to develop antibody-based HIV vaccine candidates, although additional modifications are required for the stable induction of immune responses. Importantly, since the seroconverted mice showed high viremia and high numbers of proviral DNA copies in the spleen, BM, and thymus, abundant viral production may stimulate human B-cell responses against HIV-1 and generate specific antibodies. These mice showed little or no detectable human IgG against HIV-1, as determined by Western blot analysis (data not shown), suggesting that very low levels of class-switching occurred in these mice, though further study is required.

In addition to the humoral immune responses, the induction of primary T-cell responses is critical for the study of HIV-specific immune responses and pathogenesis, as well as for vaccine development. Although we did not demonstrate the T-cell ability to respond to virus antigens, human T cells from the spleen proliferated when stimulated with anti–human CD3 antibodies (data not shown), indicating that the human T cells in the NOG mice that received transplants of hematopoietic stem cells are capable of responding to T-cell receptor–mediated signals and are expected to be able to elicit primary antigen-specific immune responses against foreign antigens. To address whether the specific T-cell responses may be induced will be one of the important studies.

In conclusion, the NOG mice that received transplants of human hematopoietic stem cells successfully achieved systemic and persistent infection with both R5-tropic and X4-tropic HIV-1, and generated humoral immune responses against HIV-1. These capacities of the hNOG mouse model may be very attractive for the study of HIV pathogenesis and humoral immune responses induced by HIV vaccine candidates.

Acknowledgments

We thank Yuetsu Tanaka of the University of Ryukyus, Tetsutaro Sata of NIID, and Shuzo Matsushita of Kumamoto University for their kind provision of mAbs to HIV-1, as well as Yukoku Tamaoka of Saiseikai Central Hospital, Toshio Akashi of Kumakiri Obstetric and Gynecologic Clinic, and Hideo Mugishima of Nihon University School of Medicine for their provision of umbilical cord blood. We also would like to express our gratitude to Ken Watanabe and Hideko Ogata of Tokyo Medical and Dental University for their skillful technical support.

This work was supported by grants from Research on Health Sciences focusing on Drug Innovation, the Japan Health Sciences Foundation.

Authorship

Contributions: S.W., K.T., N.S., M.H., and N.Y. designed the study; S.W., K.T., S.O., S.H., M.Y., Y.S., M.Z.D., and Z.Y. carried out the research; M.I. contributed live mice; S.W., K.T., and T.M. analyzed the data; N.S., M.H., and N.Y. controlled the data; S.W. wrote the paper; and all authors checked the final version of the manuscript.

Conflict-of-interest statement: The authors declare no competing financial interests.

Correspondence: Naoki Yamamoto, AIDS Research Center, National Institute of Infectious Diseases, 1-23-1 Toyama, Shinjuku-ku, Tokyo 162-8640, Japan; e-mail: nyama@nih.go.jp; Mitsuo Honda, AIDS Research Center, National Institute of Infectious Diseases, 1-23-1 Toyama, Shinjuku-ku, Tokyo 162-8640, Japan; e-mail: mhonda@nih.go.jp; and Norio Shimizu, Department of Virology, Division of Medical Science, Medical Research Institute, Tokyo Medical and Dental University, 1-5-45 Yushima, Bunkyo-ku, Tokyo 113-8519, Japan; e-mail: nshivir@tmd.ac.jp.

References

1. Letvin NL, Barouch DH, Montefiori DC. Prospects for vaccine protection against HIV-1 infection and AIDS. Annu Rev Immunol. 2002;20:73-99.
2. Namikawa R, Kaneshima H, Lieberman M, Weissman IL, McCune JM. Infection of the SCID-hu mouse by HIV-1. Science. 1988;242: 1684-1686.
3. Bonyhadi ML, Rabin L, Salimi S, et al. HIV induces thymus depletion in vivo. Nature. 1993; 363:728-732.
4. Aldrovandi GM, Feuer G, Gao L, et al. The SCID-hu mouse as a model for HIV-1 infection. Nature. 1993;363:732-736.
5. Su L, Kaneshima H, Bonyhadi M, et al. HIV-1-induced thymocyte depletion is associated with indirect cytopathogenicity and infection of progenitor cells in vivo. Immunity. 1995;2:25-36.
6. Kaneshima H, Su L, Bonyhadi ML, Connor RI, Ho DD, McCune JM. Rapid-high, syncytium-inducing isolates of human immunodeficiency virus type 1 induce cytopathicity in the human thymus of the SCID-hu mouse. J Virol. 1994;68:8188-8192.
7. Jenkins M, Hanley MB, Moreno MB, Wieder E, McCune JM. Human immunodeficiency virus-1 infection interrupts thymopoiesis and multilineage hematopoiesis in vivo. Blood. 1998;91:2672-2678.
8. Koka PS, Fraser JK, Bryson Y, et al. Human immunodeficiency virus inhibits multilineage hematopoiesis in vivo. J Virol. 1998;72:5121-5127.
9. Mosier DE, Gulizia RJ, Baird SM, Wilson DB, Spector DH, Spector SA. Human immunodeficiency virus infection of human-PBL-SCID mice. Science. 1991;251:791-794.
10. Torbett BE, Picchio G, Mosier DE. hu-PBL-SCID mice: a model for human immune function, AIDS, and lymphomagenesis. Immunol Rev. 1991;124: 139-164.
11. Ruxrungtham K, Boone E, Ford H Jr, Driscoll JS, Davey RT Jr, Lane HC. Potent activity of 2'-beta-fluoro-2',3'-dideoxyadenosine against human immunodeficiency virus type 1 infection in hu-PBL-SCID mice. Antimicrob Agents Chemother. 1996;40:2369-2374.
12. Mosier DE, Gulizia RJ, MacIsaac PD, Torbett BE, Levy JA. Rapid loss of CD4+ T cells in human-PBL-SCID mice by noncytopathic HIV isolates. Science. 1993;260:689-692.
13. Koyanagi Y, Tanaka Y, Kira J, et al. Primary human immunodeficiency virus type 1 viremia and central nervous system invasion in a novel hu-PBL-immunodeficient mouse strain. J Virol. 1997; 71:2417-2424.
14. Tary-Lehmann M, Saxon A, Lehmann PV. The human immune system in hu-PBL-SCID mice. Immunol Today. 1995;16:529-533.
15. Ito M, Hiramatsu H, Kobayashi K, et al. NOD/SCID/gamma(c)(null) mouse: an excellent recipient mouse model for engraftment of human cells. Blood. 2002;100:3175-3182.
16. Yahata T, Ando K, Nakamura Y, et al. Functional human T lymphocyte development from cord blood CD34+ cells in nonobese diabetic/Shi-scid, IL-2 receptor gamma null mice. J Immunol. 2002; 169:204-209.
17. Hiramatsu H, Nishikomori R, Heike T, et al. Complete reconstitution of human lymphocytes from cord blood CD34+ cells using the NOD/SCID/gammacnull mice model. Blood. 2003;102:873-880.
18. Matsumura T, Kametani Y, Ando K, et al. Functional CD5+ B cells develop predominantly in the spleen of NOD/SCID/gammac(null) (NOG) mice transplanted either with human umbilical cord blood, bone marrow, or mobilized peripheral blood CD34+ cells. Exp Hematol. 2003;31:789-797.
19. Shinohara K, Sakai K, Ando S, et al. A highly pathogenic simian/human immunodeficiency virus with genetic changes in cynomolgus monkey. J Gen Virol. 1999;80:1231-1240.
20. Yamakami K, Honda M, Takei M, et al. Early bone marrow hematopoietic defect in simian/human immunodeficiency virus C2/1-infected macaques and relevance to advance of disease. J Virol. 2004;78:10906-10910.
21. Nakata H, Maeda K, Miyakawa T, et al. Potent anti-R5 human immunodeficiency virus type 1 effects of a CCR5 antagonist, AK602/ONO4128/GW873140, in a novel human peripheral blood mononuclear cell nonobese diabetic-SCID, interleukin-2 receptor gamma-chain-knocked-out AIDS mouse model. J Virol. 2005;79:2087-2096.
22. Heath SL, Tew JG, Tew JG, Szakal AK, Burton GF. Follicular dendritic cells and human immunodeficiency virus infectivity. Nature. 1995;377:740-744.
23. Orenstein JM, Fox C, Wahl SM. Macrophages as a source of HIV during opportunistic infections. Science. 1997;276:1857-1861.
24. van Kooyk Y, Geijtenbeek TB. A novel adhesion pathway that regulates dendritic cell trafficking and T cell interactions. Immunol Rev. 2002;186: 47-56.
25. Taylor JR Jr, Kimbrell KC, Scoggins R, Delaney M, Wu L, Camerini D. Expression and function of chemokine receptors on human thymocytes: implications for infection by human immunodeficiency virus type 1. J Virol. 2001;75:8752-8760.
26. Bleul CC, Wu L, Hoxie JA, Springer TA, Mackay CR. The HIV coreceptors CXCR4 and CCR5 are differentially expressed and regulated on human T lymphocytes. Proc Natl Acad Sci U S A. 1997; 94:1925-1930.
27. Fais S, Lapenta C, Santini SM, et al. Human immunodeficiency virus type 1 strains R5 and X4 induce different pathogenic effects in hu-PBL-SCID mice, depending on the state of activation/differentiation of human target cells at the time of primary infection. J Virol. 1999;73:6453-6459.
28. Gartner S, Markovits P, Markovitz DM, Kaplan MH, Gallo RC, Popovic M. The role of mononuclear phagocytes in HTLV-III/LAV infection. Science. 1986;233:215-219.
29. Koyanagi Y, Miles S, Mitsuyasu RT, Merrill JE, Vinters HV, Chen IS. Dual infection of the central nervous system by AIDS viruses with distinct cellular tropisms. Science. 1987;236:819-822.
30. Gendelman HE, Orenstein JM, Baca LM, et al. The macrophage in the persistence and pathogenesis of HIV infection. AIDS. 1989;3:475-495.
31. Embretson J, Zupancic M, Ribas JL, et al. Massive covert infection of helper T lymphocytes and macrophages by HIV during the incubation period of AIDS. Nature. 1993;362:359-362.
32. Igarashi T, Brown CR, Endo Y, et al. Macrophage are the principal reservoir and sustain high virus loads in rhesus macaques after the depletion of CD4+ T cells by a highly pathogenic simian immunodeficiency virus/HIV type 1 chimera (SHIV): implications for HIV-1 infections of humans. Proc Natl Acad Sci U S A. 2001;98:658-663.
33. Mir N, Costello C, Luckit J, Lindley R. HIV-disease and bone marrow changes: a study of 60 cases. Eur J Haematol. 1989;42:339-343.
34. Moses A, Nelson J, Bagby GC Jr. The influence of human immunodeficiency virus-1 on hematopoiesis. Blood. 1998;91:1479-1495.
35. Koka PS, Jamieson BD, Brooks DG, Zack JA. Human immunodeficiency virus type 1-induced hematopoietic inhibition is independent of productive infection of progenitor cells in vivo. J Virol. 1999;73:9089-9097.
36. Koka PS, Kitchen CM, Reddy ST. Targeting c-Mpl for revival of human immunodeficiency virus type 1-induced hematopoietic inhibition when CD34+ progenitor cells are re-engrafted into a fresh stromal microenvironment in vivo. J Virol. 2004;78: 11385-11392.
37. Hillyer CD, Lackey DA 3rd, Villinger F, Winton EF, McClure HM, Ansari AA. CD34+ and CFU-GM progenitors are significantly decreased in SIVsmm9 infected rhesus macaques with minimal evidence of direct viral infection by polymerase chain reaction. Am J Hematol. 1993;43:274-278.
38. Thiebot H, Louache F, Vaslin B, et al. Early and persistent bone marrow hematopoiesis defect in simian/human immunodeficiency virus-infected macaques despite efficient reduction of viremia by highly active antiretroviral therapy during primary infection. J Virol. 2001;75:11594-11602.
39. Thiebot H, Vaslin B, Derdouch S, et al. Impact of bone marrow hematopoiesis failure on T-cell generation during pathogenic simian immunodeficiency virus infection in macaques. Blood. 2005; 105:2403-2409.

JOURNAL OF VIROLOGY, Dec. 2007, p. 13259–13264 Vol. 81, No. 23
0022-538X/07/$08.00+0 doi:10.1128/JVI.01353-07

Humanized NOD/SCID/IL2Rγ^{null} Mice Transplanted with Hematopoietic Stem Cells under Nonmyeloablative Conditions Show Prolonged Life Spans and Allow Detailed Analysis of Human Immunodeficiency Virus Type 1 Pathogenesis$^{\nabla}$

Satoru Watanabe,[1,2] Shinrai Ohta,[3] Misako Yajima,[4] Kazuo Terashima,[5] Mamoru Ito,[6] Hideo Mugishima,[7] Shigeyoshi Fujiwara,[4] Kazufumi Shimizu,[2] Mitsuo Honda,[3] Norio Shimizu,[1]* and Naoki Yamamoto[3,5]*

Department of Virology, Division of Medical Science, Medical Research Institute, Tokyo Medical and Dental University, 1-5-45 Yushima, Bunkyo-ku, Tokyo 113-8519, Japan[1]; Open Research Center for Genome and Infectious Disease Control, Nihon University School of Medicine, 30-1 Oyaguchikami-chou, Itabashi-ku, Tokyo 173-8610, Japan[2]; AIDS Research Center, National Institute of Infectious Diseases, 1-23-1 Toyama, Shinjuku-ku, Tokyo 162-8640, Japan[3]; Department of Infectious Diseases, National Research Institute for Child Health and Development, 2-10-1 Okura, Setagaya-ku, Tokyo 154-8567, Japan[4]; Department of Molecular Virology, Graduate School of Medicine, Tokyo Medical and Dental University, 1-5-45 Yushima, Bunkyo-ku, Tokyo 113-8519, Japan[5]; Central Institute for Experimental Animals, 1430 Nogawa, Miyamae-ku, Kawasaki, Kanagawa 216-0001, Japan[6]; and Department of Pediatrics and Child Health, Nihon University School of Medicine, 30-1 Oyaguchikami-chou, Itabashi-ku, Tokyo 173-8610, Japan[7]

Received 21 June 2007/Accepted 3 September 2007

In a previous study, we demonstrated that humanized NOD/SCID/IL2Rγ^{null} (hNOG) mice constructed with human hematopoietic stem cells (HSCs) allow efficient human immunodeficiency virus type 1 (HIV-1) infection. However, HIV-1 infection could be monitored for only 43 days in the animals due to their short life spans. By transplanting HSCs without any myeloablation methods, the mice successfully survived longer than 300 days with stable engraftment of human cells. The mice showed high viremia state for more than the 3 months examined, with systemic HIV-1 infection and gradual decrease of CD4$^+$ T cells analogous to that in humans. These capacities of the hNOG mice are very attractive for modeling mechanisms of AIDS progression and therapeutic strategy.

One of the main problems in the field of human immunodeficiency virus type 1 (HIV-1) research is the lack of suitable small animal models for studying the virological and pathogenic aspects of human HIV-1 infection. To overcome the drawback that HIV-1 does not replicate in rodent cells, severe combined immunodeficiency (SCID) mice, engrafted with human peripheral blood mononuclear cells (hu-PBL-SCID) (16) or human fetal thymus and liver tissue [SCID-hu (Thy/Liv)] (18), have been used for the small animal models of HIV-1 infection. However, these mouse models fall short of accurately mirroring human HIV infection because of their short infection spans (17), limited infection of lymphoid tissues (15), and partial infection to coreceptor tropic HIVs (4, 10, 13).

Considering the significant advantages of developing a mouse model for HIV-1 infection, we previously introduced a novel HIV-1 mouse model using nonobese diabetic (NOD)/SCID/interleukin-2 receptor (IL-2R) gamma chain-knocked-out (NOG) mice (22). Multilineage human cells, including T, B, NK cells, monocytes/macrophages, and dendritic cells (DCs) differentiate in the mice when transplanted with human CD34$^+$ hematopoietic stem cells (HSCs) (6, 9, 22). These mice show high levels of susceptibility to both CCR5 (R5)- and CXCR4 (X4)-tropic HIVs with intense plasma viral loads lasting for over 40 days (22). Thus, this mouse model may be valuable for the study of HIV-1 infection. However, a serious problem remains. The mice showed symptoms of a wasting condition and a hunched back 5 to 7 months after HSC transplantation, following which most of them died. This life span is not sufficient if we are to better understand HIV pathogenesis and to develop novel anti-HIV countermeasures, because more than 4 months posttransplantation is required for the development of human T cells before HIV-1 can be studied in mice.

In past studies for the construction of humanized mouse models using NOD/SCID, β2 microglobulin-deficient NOD/SCID (NOD/SCID/B2m^{null}) or NOG mice, the mice were subjected to total body irradiation or given drugs for HSC transplantation (6, 9, 11, 14, 21, 23). Since NOG mice do not develop any thymic lymphomas in contrast to NOD/SCID or NOD/SCID/B2m^{null} mice (3, 19), the irradiation might influence the reduction of their life spans. In this study, we therefore searched for optimal conditions for HSC transplantation and consequently found that in NOG mice, myeloablation procedures were not required for human cell generation. Importantly, these mice stably survived

* Corresponding author. Mailing address for Naoki Yamamoto: AIDS Research Center, National Institute of Infectious Diseases, 1-23-1 Toyama, Shinjuku-ku, Tokyo 162-8640, Japan. Phone: 81-3-5285-1111. Fax: 81-3-5285-1165. E-mail: nyama@nih.go.jp. Mailing address for Norio Shimizu: Department of Virology, Division of Medical Science, Medical Research Institute, Tokyo Medical and Dental University, 1-5-45 Yushima, Bunkyo-ku, Tokyo 113-8519, Japan. Phone and fax: 81-3-5803-5811. E-mail: nshivir@tmd.ac.jp.

$^{\nabla}$ Published ahead of print on 19 September 2007.

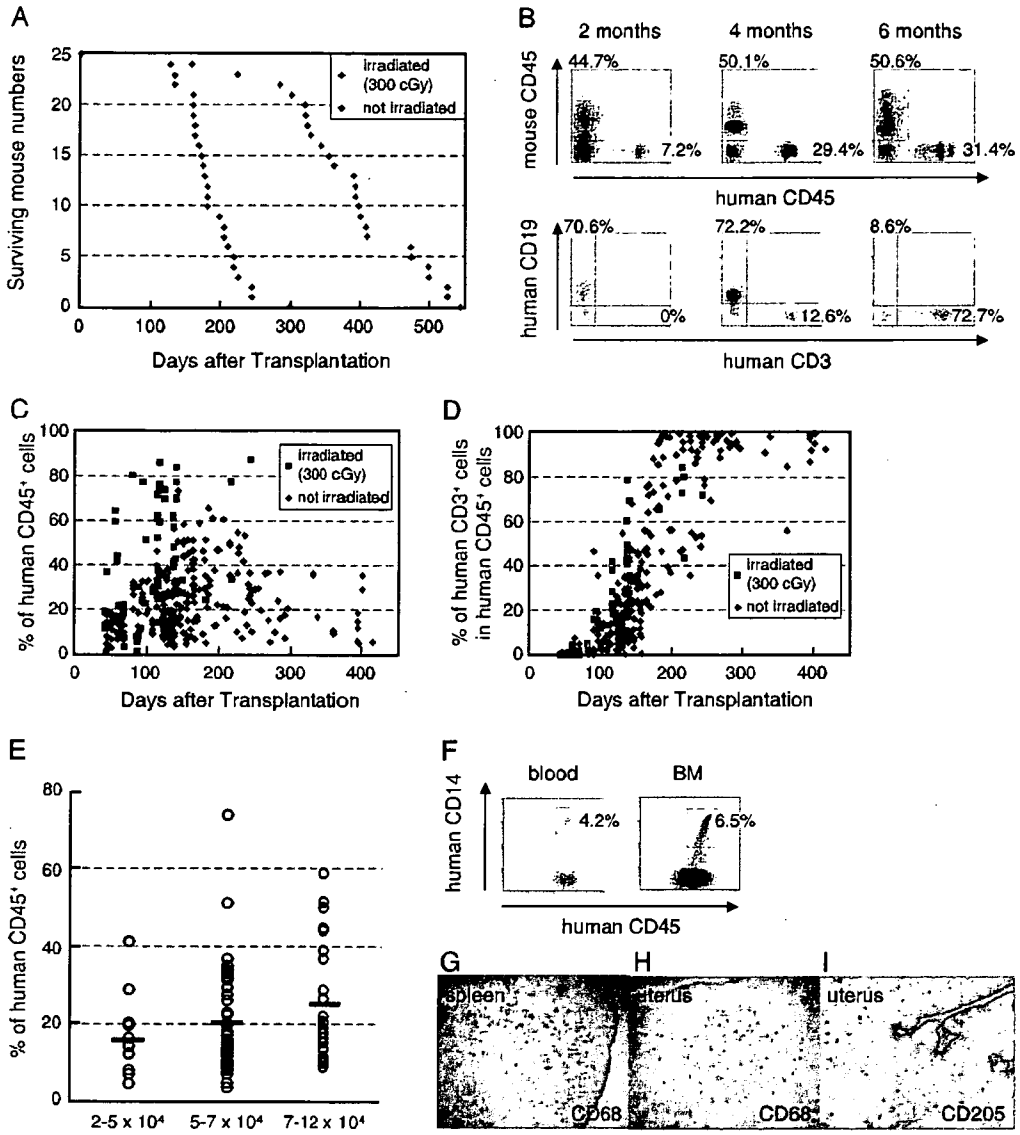

FIG. 1. Human cell generation in hematopoietic stem cell-engrafted hNOG mice with or without myeloablation. (A) Life spans of NOG mice transplanted with human stem cells after receiving 300 cGy irradiation (n = 25) or not receiving irradiation (n = 25). (B) Representative flow cytometric profiles of the mice from 2 to 6 months after transplantation without irradiation. The ratio of human to murine CD45$^+$ cells and that of human CD3$^+$ cells to CD19$^+$ cells are shown. Note that the mice generated human CD45$^+$ leukocytes that eventually developed human CD19$^+$ B cells first and then CD3$^+$ T cells. (C and D) Percentages of human CD45$^+$ cells (C) and CD3$^+$ T cells in human CD45$^+$ cells (D) in peripheral blood from 65 mice that received 300 cGy irradiation and 222 nonirradiated mice 40 to 413 days after transplantation. (E) Summary of engraftment levels in nonirradiated mice transplanted with 2×10^4 to 5×10^4 cells (n = 11), 5×10^4 to 7×10^4 cells (n = 53), or 7×10^4 to 12×10^4 (n = 30) human stem cells. Percentages of human CD45$^+$ leukocytes in peripheral blood during 4 to 5 months after transplantation were shown. The horizontal black bars indicate the averages of the groups. (F to I) Flow cytometric analysis and immunohistochemical analysis of the expression of myelomonocytic markers in nonirradiated mice 4 months after transplantation. Human CD14$^+$ monocytes/macrophages were recognized in peripheral blood and BM (F). A gate was set on the human CD45$^+$ population. Human CD68$^+$ macrophages and CD205$^+$ DCs were also detected in spleen (G) and uterus (H and I). Visualization was performed with 5-bromo-4-chloro-3-indolylphosphate (BCIP). The original magnifications were ×100 (G and H) and ×200 (I).

longer than 300 days after the HSC transplantation, which allowed further investigation of HIV-1 pathogenesis and progression to disease state in the animals.

NOG mice constructed with HSCs without myeloablation showed prolonged survival time and stable human cell generation. Six- to eight-week-old female NOG mice were obtained from the Central Institute for Experimental Animals (Kawasaki, Japan), and human cord blood-derived CD34$^+$ HSCs (2×10^4 to 12×10^4 cells) were injected intravenously with or without irradiation. As shown in Fig. 1A, most of the mice that received 300 cGy irradiation were dead within 250 days post-transplantation (mean survival time, 188 days). In contrast, more than 80% of the mice with transplanted HSCs without irradiation survived over 300 days (mean survival time, 387

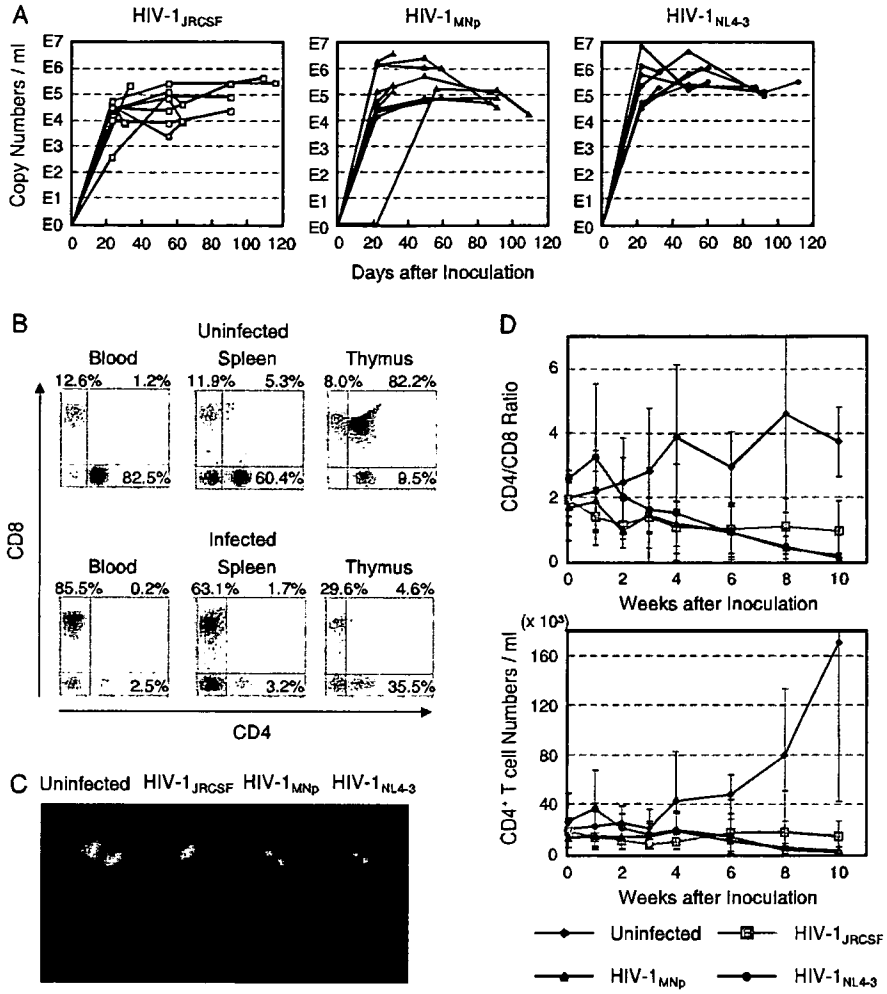

FIG. 2. Long-lasting viremia and $CD4^+$ T-cell depletion in R5- and X4-tropic HIV-1-infected hNOG mice. (A) Viral copy numbers in plasma from 29 mice intravenously inoculated with R5-tropic HIV-1_{JRCSF} (65,000 $TCID_{50}$; n = 11), X4-tropic HIV-1_{MNp} (20,000 $TCID_{50}$; n = 10), and X4-tropic HIV-1_{NL4-3} (60,000 $TCID_{50}$; n = 8). RNA viral copy numbers were measured using a real-time PCR quantification assay as previously described (22). (B) The percentages of $CD4^-$ $CD8^+$ (top left), $CD4^+$ $CD8^+$ (top right), and $CD4^+$ $CD8^-$ (bottom right) cells in blood, spleen, and thymus from a uninfected control mouse and a V-1_{NL4-3}-infected mouse (32 days postinfection). These two mice were constructed with HSCs from the same cord blood donor, and sacrificed 181 and 169 days after transplantation, respectively. A gate was set on the human $CD45^+$ population. (C) Comparison of the apparent size of mesenteric LN from uninfected mice or mice infected with HIV-1_{JRCSF} (109 days postinfection), HIV-1_{MNp} (109 days postinfection), or HIV-1_{NL4-3} (112 days postinfection). A uninfected control mouse was sacrificed 249 days after transplantation, and three HIV-1-infected mice were sacrificed 246, 246, and 249 days after transplantation. (D) Comparison of CD4/CD8 T-cell ratios and absolute $CD4^+$ T-cell numbers in peripheral blood from uninfected control mice (n = 7), R5-tropic HIV-1_{JRCSF}-infected mice (n = 7), X4-tropic HIV-1_{MNp}-infected mice (n = 5), and X4-tropic HIV-1_{NL4-3}-infected mice (n = 6). Results are expressed as means ± standard deviations (error bars).

days). These mice were successfully engrafted with HSCs, resulting first in the generation of human $CD19^+$ B cells and subsequently in the generation of human $CD3^+$ T cells (Fig. 1B). Figure 1C and D show the percentages of human $CD45^+$ leukocytes and human $CD3^+$ T cells in peripheral blood at 40 to 413 days after HSC transplantation. Up to 74% of leukocytes in peripheral blood samples were reconstituted with human cells in nonirradiated mice (mean ± standard deviation, 22.8% ± 14.0%; n = 222), and this was maintained over 400 days after transplantation (Fig. 1C). Although higher levels of human cell reconstitution were observed in the irradiated mice (45.2% ± 23.9%; n = 65) (Fig. 1C), which may be due to reduction of absolute numbers of murine cells by destruction of their progenitor cells in bone marrow (BM), human $CD3^+$ T cells developed with similar kinetics between the two groups (Fig. 1D). Figure 1E shows the engraftment efficiency of NOG mice transplanted with different numbers of HSCs without irradiation. More than 2×10^4 HSCs could be stably engrafted, and the levels of human cell reconstitution increased relative to the number of transplanted cells.

We further analyzed the development of human monocytes, macrophages, and DCs in the mice with transplanted HSCs without irradiation. Human $CD14^+$ monocytes were detected in peripheral blood and BM using flow cytometry (Fig. 1F), and many human $CD68^+$ macrophages were observed in various organs, including spleen (Fig. 1G), uterus (Fig. 1H), ovary, and lung (data not shown). Human $CD205^+$ DCs were also detected in spleen (data not shown) and uterus (Fig. 1I). These

TABLE 1. CD4/CD8 ratios in peripheral blood and spleen and $CD4^+$ $CD8^+$ cells in thymus of groups of uninfected and HIV-1-infected mice[a]

Group and mouse identification no.	No. of days after inoculation	CD4/CD8 ratio		% of $CD4^+$ $CD8^+$ cells in thymus	No. of RNA viral copies/ml
		Blood	Spleen		
Uninfected control group (n = 15)		2.92 ± 1.68	2.78 ± 1.46	67.8 ± 20.5	
$HIV\text{-}1_{JRCSF}$-infected group					
1	30	1.86	0.88	77.1	9,078
2	30	0.46	0.53	12.5	7,703
3	33	2.61	2.17	85.7	223,020
4	63	0.17	0.27	25.5	9,965
5	63	0.36	0.44	27.2	8,734
6	63	0.18	0.88	69.6	42,198
7	90	0.03	0.37	82.5	24,441
8	90	0.30	0.79	84.6	24,454
9	90	1.77	1.55	56.9	80,636
10	109	0.20	0.17	43.4	470,392
11	116	0.09	0.78	11.8	299,080
$HIV\text{-}1_{MNp}$-infected group					
1	31	0.82	0.44	34.6	3,709,520
2	31	1.02	0.61	90.2	219,971
3	31	1.64	1.57	78.2	135,592
4	59	0.21	0.38	35.4	78,848
5	59	0.10	0.07	77.0	1,039,716
6	87	0.20	0.40	0.5	49,080
7	87	0.19	0.08	11.7	121,817
8	91	0.04	0.04	82.9	30,706
9	91	0.28	0.10	1.2	7,407
10	109	0.00	0.21	2.8	17,310
$HIV\text{-}1_{NL4\text{-}3}$-infected group					
1	32	1.01	0.81	64.5	195,375
2	32	0.03	0.05	4.6	770,721
3	60	0.21	0.13	3.9	1,108,003
4	60	0.14	ND[b]	ND	328,375
5	87	0.03	0.04	1.0	201,207
6	92	0.03	0.17	11.1	90,831
7	92	0.03	0.03	1.4	135,514
8	112	0.30	0.23	0.2	325,202

[a] Twenty-nine mice inoculated with R5-tropic $HIV\text{-}1_{JRCSF}$ (n = 11), X4-tropic $HIV\text{-}1_{MNp}$ (n = 10), or X4-tropic $HIV\text{-}1_{NL4\text{-}3}$ (n = 8) were sacrificed 161 to 249 days after HSC transplantation. Fifteen uninfected control mice were sacrificed 174 to 249 days after transplantation, and results for the control group are expressed as means ± standard deviations.

[b] ND, not determined because of a lack of cells.

observations were similar to those seen in irradiated mice as shown in our previous report (22). Thus, humanized NOG (hNOG) mice without any myeloablation procedures allowed sufficient development of human cells to study HIV-1 pathogenesis.

hNOG mice induced systemic and long-lasting HIV-1 infection with $CD4^+$ T-cell depletion. We prepared 29 stem cell-transplanted hNOG mice and inoculated them intravenously with a high dose of R5-tropic $HIV\text{-}1_{JRCSF}$ (65,000 50% tissue culture infective doses [$TCID_{50}$]), X4-tropic $HIV\text{-}1_{MNp}$ (20,000 $TCID_{50}$), or X4-tropic $HIV\text{-}1_{NL4\text{-}3}$ (60,000 $TCID_{50}$) at 122 to 150 days posttransplantation. Then, plasma viral RNA copy numbers were measured at successive time points. The mice showed marked, long-lasting viremia state for more than 3 months, reaching the highest levels of 3.0×10^5 copies/ml from $HIV\text{-}1_{JRCSF}$-infected mice, 3.7×10^6 copies/ml from $HIV\text{-}1_{MNp}$-infected mice, and 7.8×10^6 copies/ml from $HIV\text{-}1_{NL4\text{-}3}$-infected mice (Fig. 2A). None of the mice weakened or died as a result of HIV-1 infection throughout the entire follow-up period.

All the mice were sacrificed within 4 months postinfection, and the percentages of $CD4^+$ and $CD8^+$ cells in lymphoid tissues were analyzed by flow cytometry. In a representative HIV-1-infected mouse, as shown in Fig. 2B, CD4/CD8 ratios in blood and spleen significantly decreased with apparent loss of $CD4^+$ $CD8^+$ double positive thymocytes. The size of lymphoid tissues, such as thymus and lymph node (LN), in the HIV-1-infected mice was very small compared with uninfected mice (Fig. 2C), suggesting that they shrank as a result of HIV-1 infection. Table 1 illustrates the overall profile of CD4/CD8 ratios in blood and spleen and the percentages of $CD4^+$ $CD8^+$ thymocytes from the 29 HIV-1-infected mice. Most of the mice, both R5- and X4-tropic and HIV-1 infected, had reduced CD4/CD8 ratios in blood and spleen compared with unin-

TABLE 2. Comparison of DNA proviral copies in various organs from HIV-1-infected mice[a]

Organ	No. of HIV-1 DNA copies/100 ng DNA in mice infected with[b]:		
	HIV-1_{JRCSF}	HIV-1_{MNp}	HIV-1_{NL4-3}
Peripheral blood	60	6	UD
Spleen	793	1,143	2,115
Bone marrow	2,432	656	584
Thymus	23	2,074	17,374
Lymph node	2,103	942	2,115
Lung	239	145	177
Liver	74	49	12
Small intestine	ND	6	9
Ovary	24	122	10
Uterus	14	5	16
Rectum	UD	16	11
Heart	9	UD	UD
Skin	UD	UD	138
Brain	UD	2	UD
Eyeball	3	25	UD

[a] Viral DNA was extracted from various organs of mice infected with HIV-1_{JRCSF} (33 days postinfection), HIV-1_{MNp} (59 days postinfection), and HIV-1_{NL4-3} (60 days postinfection). Determination of HIV-1 DNA copy numbers was performed by real-time PCR assay as previously described (22).
[b] UD, undetected; ND, not done.

fected control mice. On the other hand, a reduction of $CD4^+$ $CD8^+$ thymocytes was observed especially in X4-tropic HIV-1-infected mice, which seemed to correlate with the predominant expression of CXCR4 on the thymocytes as we previously described (22). Interestingly, two mice that were infected with HIV-1_{MNp} (mouse identification number 5 and 8) maintained their high percentages of $CD4^+$ $CD8^+$ thymocytes in spite of significant CD4/CD8 decline in their blood and spleen, suggesting no direct relationship between thymic T-cell depletion and CD4/CD8 decrease in peripheral blood or spleen by HIV-1 infection.

In one mouse from each R5- and X4-tropic HIV-infected group, HIV-1 proviral DNA copy numbers in various organs were measured by real-time PCR assay (Table 2). High HIV DNA copy numbers were detected in the spleen, BM, and LN of the R5-tropic HIV-1-infected mouse and in the thymus, spleen, and LN of the X4-tropic HIV-1-infected mice. In addition, HIV DNA copies were detectable in various other organs, including the lung, liver, ovary, and uterus. The fact that many human $CD68^+$ macrophages, the source of HIV-1 throughout the body (7, 8), were recognized in these organs (22) (Fig. 1H) may help explain the susceptibility of these organs to HIV-1.

To further investigate the progression of $CD4^+$ T-cell depletion by HIV-1 infection, 25 mice 120 to 151 days after HSC transplantation were randomly separated into groups of uninfected control mice (n = 7), HIV-1_{JRCSF}-inoculated mice (n = 7), HIV-1_{MNp}-inoculated mice (n = 5), and HIV-1_{NL4-3}-inoculated mice (n = 6), and then CD4/CD8 ratios and absolute $CD4^+$ T-cell numbers in peripheral blood were monitored at regular intervals. X4-tropic HIV-infected mice showed gradual decreases of their CD4/CD8 ratios and $CD4^+$ T-cell numbers, which eventually resulted in an almost complete depletion from peripheral blood (Fig. 2D). While $CD4^+$ T-cell depletion was also seen in R5-tropic HIV-infected mice, this was less prominent compared with X4-tropic HIV-1-infected mice (Fig. 2D). This pattern of R5- versus X4-tropic HIV-1 infection seems to correlate with the general observation that the emergence of X4-tropic HIVs accelerates $CD4^+$ T-cell decline and disease progression in HIV patients (12, 20).

In this study, we successfully prolonged the life span of hNOG mice by improving the HSC transplantation method and further clarified characteristics of HIV-1 infection in the mice including the following: (i) high levels of viremia lasting over 3 months, (ii) $CD4^+$ T-cell depletion in peripheral blood and spleen regardless of thymic T-cell loss, (iii) systemic HIV-1 infection not only in lymphoid tissues but also in various other organs, and (iv) a different rate of $CD4^+$ T-cell depletion for R5- versus X4-tropic HIV-1 strains. Recently, several studies on HIV-1 infection in $Rag2^{-/-}$ $\gamma c^{-/-}$ mice, transplanted with HSCs at birth, have also been reported (1, 2, 5, 24). The mice showed high susceptibility to both R5- and X4-tropic HIVs and long-term viremia with $CD4^+$ T-cell depletion, which is partly similar to our present results. However, the efficiency of human cell generation in $Rag2^{-/-}$ $\gamma c^{-/-}$ mice strongly depends on the dose of irradiation, and levels of chimerism in mice are not stable even receiving 550 to 750 cGy irradiation, which does eventually induces reduction of their life spans (5). In contrast, very stable engraftment of HSCs and subsequent human cell generation were noted in our hNOG mice even without any myeloablation procedures. Their long life spans and long-term human cell reconstitution allowed persistent HIV-1 infections mirroring HIV-1 infections in humans. Thus, this hNOG mouse system is a very useful tool as an advanced mouse model for the study of AIDS progression and long-term evaluation of new anti-HIV-1 drugs.

We thank Tomohiro Morio, Ken Watanabe, and Eiko Ogata of Tokyo Medical and Dental University for their helpful comments and skillful technical support. We are also grateful to Yukari Sasaki and Kazuhiro Takimoto of the National Institute of Infectious Diseases and Teruaki Tanaka and Junichi Fujita of the Nihon University School of Medicine for their management of animals. Human umbilical cord blood samples were obtained from the Tokyo Cord Blood Bank of the Nihon University School of Medicine.

This work was supported by a grant from the Ministry of Education, Culture, Sports, Science, and Technology to promote open research for young academics and specialists.

REFERENCES

1. **Baenziger, S., R. Tussiwand, E. Schlaepfer, L. Mazzucchelli, M. Heikenwalder, M. O. Kurrer, S. Behnke, J. Frey, A. Oxenius, H. Joller, A. Aguzzi, M. G. Manz, and R. F. Speck.** 2006. Disseminated and sustained HIV infection in $CD34^+$ cord blood cell-transplanted $Rag2^{-/-}$ $\gamma c^{-/-}$ mice. Proc. Natl. Acad. Sci. USA 103:15951–15956.
2. **Berges, B. K., W. H. Wheat, B. E. Palmer, E. Connick, and R. Akkina.** 2006. HIV-1 infection and CD4 T cell depletion in the humanized $Rag2^{-/-}$ $\gamma c^{-/-}$ (RAG-hu) mouse model. Retrovirology 3:76.
3. **Christianson, S. W., D. L. Greiner, R. A. Hesselton, J. H. Leif, E. J. Wagar, I. B. Schweitzer, T. V. Rajan, B. Gott, D. C. Roopenian, and L. D. Shultz.** 1997. Enhanced human $CD4^+$ T cell engraftment in beta2-microglobulin-deficient NOD-scid mice. J. Immunol. 158:3578–3586.
4. **Fais, S., C. Lapenta, S. M. Santini, M. Spada, S. Parlato, M. Logozzi, P. Rizza, and F. Belardelli.** 1999. Human immunodeficiency virus type 1 strains R5 and X4 induce different pathogenic effects in hu-PBL-SCID mice, depending on the state of activation/differentiation of human target cells at the time of primary infection. J. Virol. 73:6453–6459.
5. **Gorantla, S., H. Sneller, L. Walters, J. G. Sharp, S. J. Pirruccello, J. T. West, C. Wood, S. Dewhurst, H. E. Gendelman, and L. Poluektova.** 2007. Human immunodeficiency virus type 1 pathobiology studied in humanized BALB/c-$Rag2^{-/-}\gamma_c^{-/-}$ mice. J. Virol. 81:2700–2712.
6. **Hiramatsu, H., R. Nishikomori, T. Heike, M. Ito, K. Kobayashi, K. Katamura, and T. Nakahata.** 2003. Complete reconstitution of human lym-

phocytes from cord blood CD34$^+$ cells using the NOD/SCID/γ_c^{null} mice model. Blood **102**:873–880.

7. **Igarashi, T., C. R. Brown, Y. Endo, A. Buckler-White, R. Plishka, N. Bischofberger, V. Hirsch, and M. A. Martin.** 2001. Macrophage are the principal reservoir and sustain high virus loads in rhesus macaques after the depletion of CD4$^+$ T cells by a highly pathogenic simian immunodeficiency virus/HIV type 1 chimera (SHIV): implications for HIV-1 infections of humans. Proc. Natl. Acad. Sci. USA **98**:658–663.
8. **Igarashi, T., O. K. Donau, H. Imamichi, M. J. Dumaurier, R. Sadjadpour, R. J. Plishka, A. Buckler-White, C. Buckler, A. F. Suffredini, H. C. Lane, J. P. Moore, and M. A. Martin.** 2003. Macrophage-tropic simian/human immunodeficiency virus chimeras use CXCR4, not CCR5, for infections of rhesus macaque peripheral blood mononuclear cells and alveolar macrophages. J. Virol. **77**:13042–13052.
9. **Ito, M., H. Hiramatsu, K. Kobayashi, K. Suzue, M. Kawahata, K. Hioki, Y. Ueyama, Y. Koyanagi, K. Sugamura, K. Tsuji, T. Heike, and T. Nakahata.** 2002. NOD/SCIDγ_c^{null} mouse: an excellent recipient mouse model for engraftment of human cells. Blood **100**:3175–3182.
10. **Kaneshima, H., L. Su, M. L. Bonyhadi, R. I. Connor, D. D. Ho, and J. M. McCune.** 1994. Rapid-high, syncytium-inducing isolates of human immunodeficiency virus type 1 induce cytopathicity in the human thymus of the SCID-hu mouse. J. Virol. **68**:8188–8192.
11. **Kollet, O., A. Peled, T. Byk, H. Ben-Hur, D. Greiner, L. Shultz, and T. Lapidot.** 2000. β2 Microglobulin-deficient (B2m^{null}) NOD/SCID mice are excellent recipients for studying human stem cell function. Blood **95**:3102–3105.
12. **Koot, M., I. P. Keet, A. H. Vos, R. E. de Goede, M. T. Roos, R. A. Coutinho, F. Miedema, P. T. Schellekens, and M. Tersmette.** 1993. Prognostic value of HIV-1 syncytium-inducing phenotype for rate of CD4$^+$ cell depletion and progression to AIDS. Ann. Intern. Med. **118**:681–688.
13. **Koyanagi, Y., Y. Tanaka, J. Kira, M. Ito, K. Hioki, N. Misawa, Y. Kawano, K. Yamasaki, R. Tanaka, Y. Suzuki, Y. Ueyama, E. Terada, T. Tanaka, M. Miyasaka, T. Kobayashi, Y. Kumazawa, and N. Yamamoto.** 1997. Primary human immunodeficiency virus type 1 viremia and central nervous system invasion in a novel hu-PBL-immunodeficient mouse strain. J. Virol. **71**:2417–2424.
14. **Matsumura, T., Y. Kametani, K. Ando, Y. Hirano, I. Katano, R. Ito, M. Shiina, H. Tsukamoto, Y. Saito, Y. Tokuda, S. Kato, M. Ito, K. Motoyoshi, and S. Habu.** 2003. Functional CD5$^+$ B cells develop predominantly in the spleen of NOD/SCID/γc^{null} (NOG) mice transplanted either with human umbilical cord blood, bone marrow, or mobilized peripheral blood CD34$^+$ cells. Exp. Hematol. **31**:789–797.
15. **McCune, J., H. Kaneshima, J. Krowka, R. Namikawa, H. Outzen, B. Peault, L. Rabin, C. C. Shih, E. Yee, M. Lieberman, I. Weissman, and L. Shultz.** 1991. The SCID-hu mouse: a small animal model for HIV infection and pathogenesis. Annu. Rev. Immunol. **9**:399–429.
16. **Mosier, D. E., R. J. Gulizia, S. M. Baird, D. B. Wilson, D. H. Spector, and S. A. Spector.** 1991. Human immunodeficiency virus infection of human-PBL-SCID mice. Science **251**:791–794.
17. **Mosier, D. E., R. J. Gulizia, P. D. MacIsaac, B. E. Torbett, and J. A. Levy.** 1993. Rapid loss of CD4$^+$ T cells in human-PBL-SCID mice by noncytopathic HIV isolates. Science **260**:689–692.
18. **Namikawa, R., H. Kaneshima, M. Lieberman, I. L. Weissman, and J. M. McCune.** 1988. Infection of the SCID-hu mouse by HIV-1. Science **242**: 1684–1686.
19. **Shultz, L. D., P. A. Schweitzer, S. W. Christianson, B. Gott, I. B. Schweitzer, B. Tennent, S. McKenna, L. Mobraaten, T. V. Rajan, D. L. Greiner, et al.** 1995. Multiple defects in innate and adaptive immunologic function in NOD/LtSz-scid mice. J. Immunol. **154**:180–191.
20. **Tersmette, M., R. A. Gruters, F. de Wolf, R. E. de Goede, J. M. Lange, P. T. Schellekens, J. Goudsmit, H. G. Huisman, and F. Miedema.** 1989. Evidence for a role of virulent human immunodeficiency virus (HIV) variants in the pathogenesis of acquired immunodeficiency syndrome: studies on sequential HIV isolates. J. Virol. **63**:2118–2125.
21. **Ueda, T., H. Yoshino, K. Kobayashi, M. Kawahata, Y. Ebihara, M. Ito, S. Asano, T. Nakahata, and K. Tsuji.** 2000. Hematopoietic repopulating ability of cord blood CD34$^+$ cells in NOD/Shi-*scid* mice. Stem Cells **18**:204–213.
22. **Watanabe, S., K. Terashima, S. Ohta, S. Horibata, M. Yajima, Y. Shiozawa, M. Z. Dewan, Z. Yu, M. Ito, T. Morio, N. Shimizu, M. Honda, and N. Yamamoto.** 2007. Hematopoietic stem cell-engrafted NOD/SCID/IL2Rγ^{null} mice develop human lymphoid systems and induce long-lasting HIV-1 infection with specific humoral immune responses. Blood **109**:212–218.
23. **Yahata, T., K. Ando, Y. Nakamura, Y. Ueyama, K. Shimamura, N. Tamaoki, S. Kato, and T. Hotta.** 2002. Functional human T lymphocyte development from cord blood CD34$^+$ cells in nonobese diabetic/Shi-*scid*, IL-2 receptor γ null mice. J. Immunol. **169**:204–209.
24. **Zhang, L., G. I. Kovalev, and L. Su.** 2007. HIV-1 infection and pathogenesis in a novel humanized mouse model. Blood **109**:2978–2981.

JOURNAL OF VIROLOGY, May 2007, p. 5202–5211 Vol. 81, No. 10
0022-538X/07/$08.00+0 doi:10.1128/JVI.02881-06

Long-Term Control of Simian Immunodeficiency Virus Replication with Central Memory CD4$^+$ T-Cell Preservation after Nonsterile Protection by a Cytotoxic T-Lymphocyte-Based Vaccine$^\nabla$

Miki Kawada,[1,2] Tetsuo Tsukamoto,[1,3] Hiroyuki Yamamoto,[1,3] Akiko Takeda,[1] Hiroko Igarashi,[3] David I. Watkins,[4] and Tetsuro Matano[1,3,5]*

International Research Center for Infectious Diseases, The Institute of Medical Science, University of Tokyo, 4-6-1 Shirokanedai, Minato-ku, Tokyo 108-8639, Japan[1]; Department of Infectious Diseases, Graduate School of Medicine, University of Tokyo, 7-3-1 Hongo, Bunkyo-ku, Tokyo 113-0033, Japan[2]; Department of Microbiology, Graduate School of Medicine, University of Tokyo, 7-3-1 Hongo, Bunkyo-ku, Tokyo 113-0033, Japan[3]; Wisconsin National Primate Research Center, University of Wisconsin—Madison, 555 Science Drive, Madison, Wisconsin 53711[4]; and AIDS Research Center, National Institute of Infectious Diseases, 1-23-1 Toyama, Shinjuku-ku, Tokyo 162-8640, Japan[5]

Received 30 December 2006/Accepted 25 February 2007

Induction of virus-specific CD8$^+$ cytotoxic T-lymphocyte (CTL) responses is a promising strategy for AIDS vaccine development. However, it has remained unclear if or how long-term viral containment and disease control are attainable by CTL-based nonsterile protection. Here, we present three rhesus macaques that successfully maintained Env-independent vaccine-based control of simian immunodeficiency virus (SIV) mac239 replication without disease progression for more than 3 years. SIV-specific neutralizing antibody induction was inefficient in these controllers. Vaccine-induced Gag-specific CTLs were crucial for the chronic as well as the primary viral control in one of them, whereas those Gag-specific CTL responses became undetectable and CTLs specific for SIV antigens other than Gag, instead, became predominant in the chronic phase in the other two controllers. A transient CD8$^+$ cell depletion experiment 3 years postinfection resulted in transient reappearance of plasma viremia in these two animals, suggesting involvement of the SIV non-Gag-specific CTLs in the chronic SIV control. This sustained, neutralizing antibody-independent viral control was accompanied with preservation of central memory CD4$^+$ T cells in the chronic phase. Our results suggest that prophylactic CTL vaccine-based nonsterile protection can result in long-term viral containment by adapted CTL responses for AIDS prevention.

Human immunodeficiency virus (HIV) and simian immunodeficiency virus (SIV) infections induce acute, massive depletion of CCR5$^+$ CD4$^+$ effector memory T cells from mucosal effector sites. This is followed by chronic immune activation with gradual immune disruption leading to AIDS (7, 15, 20, 25, 26, 33, 34). Acute depletion has an impact on disease course but does not dictate everything that happens in the chronic phase (7, 26). It has also been suggested that persistent viral replication-associated chronic immune activation may be critical for AIDS progression.

Virus-specific CD8$^+$ cytotoxic T-lymphocyte (CTL) responses are crucial for control of HIV and SIV replication (3, 8, 12, 18, 24, 29). Several vaccine regimens eliciting virus-specific CTL responses have been developed and evaluated in macaque AIDS models (6, 21). Some of them have shown protective efficacies leading to viremia control in a model of X4-tropic simian-human immunodeficiency virus (SHIV) infections (1, 16, 22, 23, 28, 31). However, assessment of the ability of vaccines to ameliorate disease progression requires analysis in macaque models of R5-tropic SIV infection (5). Although most CTL-based vaccine trials using rigorous SIV challenges in Indian rhesus macaques have failed, some of them have shown amelioration of acute memory CD4$^+$ T-cell depletion in the vaccinated animals with reduction in viral loads out to a year postinfection (4, 13, 19, 35). These findings have suggested that there may be a clinical benefit conferred by CTL-based AIDS vaccines. Unfortunately, it is still unclear as to how nonsterile protection conferred by prophylactic CTL-based vaccines can result in long-term viral containment and disease control.

We have previously developed a CTL-eliciting AIDS vaccine regimen using a DNA-prime/Gag-expressing Sendai virus (SeV-Gag) vector-boost (16, 32). Our regimen does not utilize Env immunogen that may induce neutralizing antibodies, although this antigen has been used in most of the vaccines except for a few cases (16, 31, 35). We have evaluated efficacy of this Env-independent vaccine against SIVmac239 challenge in Burmese rhesus macaques and found neutralizing antibody-independent, CTL-based control of primary SIV replication in five of eight vaccinees (17). In the present study, we have followed these macaques to examine if long-term viral containment without disease progression is possible by prophylactic CTL-based AIDS vaccines.

MATERIALS AND METHODS

Animal experiments. Twelve Burmese rhesus macaques (*Macaca mulatta*) used in our previous SIVmac239 challenge experiment (17) were followed in the

* Corresponding author. Mailing address: International Research Center for Infectious Diseases, The Institute of Medical Science, The University of Tokyo, 4-6-1 Shirokanedai, Minato-ku, Tokyo 108-8639, Japan. Phone: 81-3-6409-2078. Fax: 81-3-6409-2076. E-mail: matano@m.u-tokyo.ac.jp.

$^\nabla$ Published ahead of print on 7 March 2007.

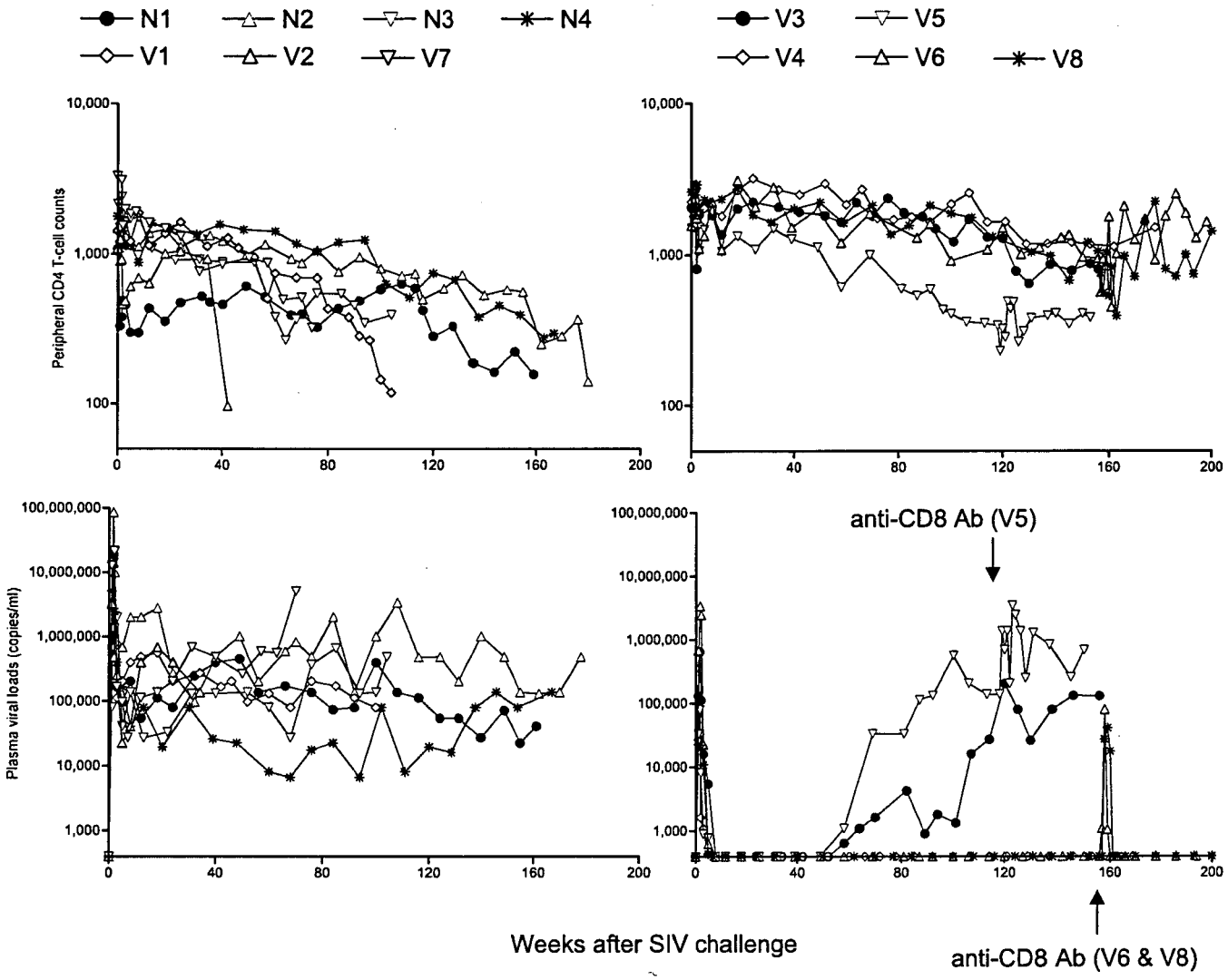

FIG. 1. Follow-up of the macaques after SIVmac239 challenge. Upper panels, peripheral CD4$^+$ T-cell counts (cells/μl); lower panels, plasma viral loads (viral RNA copies/ml plasma); left panels, the seven noncontrollers; right panels, the five controllers. All seven noncontrollers developed AIDS and were euthanized during the observation period (Table 1). Macaques V5, V6, and V8 received anti-CD8 antibody treatment starting from week 118, week 156, and week 156, respectively.

present study. These macaques were maintained in accordance with the Guideline for Laboratory Animals of the National Institute of Infectious Diseases and the National Institute of Biomedical Innovation. Four of them were naive, whereas the other eight macaques received a DNA vaccine followed by a single boost with SeV-Gag before an intravenous SIVmac239 challenge. The DNA, CMV-SHIVdEN, used for the vaccination was constructed from an *env*- and *nef*-deleted $SHIV_{MD14YE}$ molecular clone DNA (30) and has the genes encoding SIVmac239 Gag, Pol, Vif, and Vpx, SIVmac239-HIV-1_{DH12} chimeric Vpr, and HIV-1_{DH12} Tat and Rev as described previously (17). At the DNA vaccination, animals received 5 mg of CMV-SHIVdEN DNA intramuscularly. Six weeks after the DNA prime, animals intranasally received a single boost with 1×10^8 cell infectious units of replication-competent SeV-Gag (V1, V2, V3, and V4) or 6×10^9 cell infectious units of F-deleted replication-defective F(-)SeV-Gag (9, 14, 32). Approximately 3 months after the boost, animals were challenged intravenously with 1,000 50% tissue culture infective doses ($TCID_{50}$) of SIVmac239 (11).

For CD8$^+$ cell depletion, animals received a single intramuscular inoculation of 10 mg/kg of body weight of monoclonal anti-CD8 antibody (cM-T807) provided by Centocor (Malvern, PA) followed by three intravenous inoculations of 5 mg/kg cM-T807 on days 3, 7, and 10 after the first inoculation. The anti-CD8 antibody administration started at week 118 in macaque V5 and at week 156 in macaques V6 and V8. CD8$^+$ T-cell depletion in peripheral blood was confirmed by immunostaining using fluorescein isothiocyanate-conjugated anti-human CD8 antibody (DK25; Dako, Kyoto, Japan).

All the noncontrollers were euthanized when they showed typical signs of AIDS, such as reduction in peripheral CD4$^+$ T-cell counts, loss of body weight, diarrhea, and general weakness. Autopsy revealed lymphoatrophy or post-persistent generalized lymphadenopathy conditions consistent with AIDS.

Quantitation of plasma viral loads. Plasma RNA was extracted using the High Pure viral RNA kit (Roche Diagnostics, Tokyo, Japan). Serial fivefold dilutions of RNA samples were amplified in quadruplicate by reverse transcription and nested PCR using SIV *gag*-specific primers to determine the endpoint. Plasma SIV RNA levels were calculated according to the Reed-Muench method as described previously (17). The lower limit of detection is approximately 4×10^2 copies/ml.

Measurement of virus-specific neutralizing titers. Serial twofold dilutions of heat-inactivated plasma were prepared in duplicate and mixed with 10 $TCID_{50}$ of SIVmac239. In each mixture, 5 μl of diluted plasma was incubated with 5 μl of virus. After a 45-min incubation at room temperature, each 10-μl mixture was added to 5×10^4 MT4 cells in a well of a 96-well plate. After 12 days of culture, supernatants were harvested. Progeny virus production in the supernatants was examined by enzyme-linked immunosorbent assay for detection of SIV p27 core antigen (Beckman-Coulter, Tokyo, Japan) to determine the 100% neutralizing endpoint. The lower limit of detection is a titer of 1:2.

TABLE 1. Summary of responses in macaques challenged with SIVmac239

Macaque group and no.	MHC-I haplotype[a]	VL		Status[c]	CD4 count[d] at euthanasia	Opportunistic infection at autopsy[e]
		Set point[b]	After wk 60			
Unvaccinated noncontrollers						
N1	*90-088-Ij*	$>10^4$	$>10^4$	Euthanized at wk 161	158	
N2	*90-120-Ia*	$>10^4$	$>10^4$	Euthanized at wk 180	141	PCP
N3	*90-122-Ie*	$>10^4$	$>10^4$	Euthanized at wk 104	393	
N4	*90-010-Id*	$>10^4$	$>10^4$	Euthanized at wk 167	296	CMV
Vaccinated noncontrollers						
V1	*90-088-Ij*	$>10^4$	$>10^4$	Euthanized at wk 105	119	
V2	*90-120-Ib*	$>10^4$		Euthanized at wk 42	97	PCP
V7	*90-122-Ie*	$>10^4$	$>10^4$	Euthanized at wk 77	323	
Vaccinated transient controllers						
V3	*90-120-Ia*	<400	$>10^3$	Alive >3 yr		
V5	*90-120-Ia*	<400	$>10^4$	Euthanized at wk 154*	384	
Vaccinated sustained controllers						
V4	*90-120-Ia*	<400	<400	Alive >3 yr		
V6	*90-122-Ie*	<400	<400	Alive >3 yr*		
V8	*90-010-Id*	<400	<400	Alive >3 yr*		

[a] MHC-I haplotype was determined by reference strand-mediated conformation analysis as described previously (2, 17). MHC class I haplotypes *90-120-Ia* and *90-120-Ib* are derived from breeder R-90-120, *90-122-Ie* is from R-90-122, *90-010-Id* is from R-90-010, and *90-088-Ij* is from R-90-088.

[b] Plasma viral load (VL, in RNA copies/ml plasma) around week 12.

[c] All seven noncontrollers exhibited reduction in peripheral CD4 T-cell count, loss of body weight, and general weakness and were euthanized and subjected to autopsy to be confirmed as AIDS. Macaques V5, V6, and V8 (indicated by asterisks) were administered an anti-CD8 antibody for CD8 cell depletion at weeks 118, 156, and 156, respectively.

[d] Peripheral CD4 T-cell counts.

[e] PCP, pneumocystis pneumonia; CMV, cytomegalovirus infection.

Measurement of virus-specific CTL responses. We measured virus-specific $CD8^+$ T-cell levels by flow cytometric analysis of gamma interferon (IFN-γ) induction after specific stimulation as described previously (17). In brief, peripheral blood mononuclear cells (PBMCs) were cocultured with autologous herpesvirus papio-immortalized B-lymphoblastoid cell lines infected with a vaccinia virus vector expressing SIVmac239 Gag for Gag-specific stimulation or a vesicular stomatitis virus G protein (VSV-G)-pseudotyped SIVGP1 for SIV-specific stimulation. The pseudotyped virus was obtained by cotransfection of COS-1 cells with a VSV-G expression plasmid and the SIVGP1 DNA, an *env*- and *nef*-deleted SHIV molecular clone DNA. Intracellular IFN-γ staining was performed using a CytofixCytoperm kit (Becton Dickinson, Tokyo, Japan). Peridinin chlorophyll protein-conjugated anti-human CD8, allophycocyanin-conjugated anti-human CD3, and phycoerythrin-conjugated anti-human IFN-γ antibodies (Becton Dickinson) were used. Specific T-cell levels were calculated by subtracting nonspecific $IFN\text{-}\gamma^+$ T-cell frequencies from those after Gag-specific or SIV-specific stimulation. Specific T-cell levels less than 100 cells per million PBMCs are considered negative.

Immunostaining of $CD4^+$ T-cell memory subsets. Frozen stocks of PBMCs were thawed and subjected to immunofluorescent staining by using fluorescein isothiocyanate-conjugated anti-human CD28, phycoerythrin-conjugated anti-human CD95, peridinin chlorophyll-conjugated anti-human CD4, and allophycocyanin-conjugated anti-human CD3 monoclonal antibodies (Becton Dickinson). Memory and central memory subsets of $CD4^+$ T cells were delineated by $CD95^+$ and $CD28^+$ $CD95^+$ phenotypes, respectively, as described previously (27).

Statistical analysis. Central memory $CD4^+$ T-cell counts just before SIV challenge (at week zero) were not significantly different between the noncontrollers (n = 7) and the controllers (n = 5) by unpaired t test. We calculated ratios of the counts at week 12 to week 0, week 70 to week 0, and week 70 to week 12 in each animal and performed an unpaired t test and nonparametric Mann-Whitney U-test between the noncontrollers and the controllers by using Prism software version 4.03 (GraphPad Software, Inc., San Diego, CA).

RESULTS

Long-term viral containment without disease progression in the sustained controllers. We followed up on our vaccinated Burmese rhesus macaques used in the previous trial (17). These macaques were vaccinated using a DNA prime–SeV-Gag boost, and they were challenged with SIVmac239. Five of eight vaccinees controlled viral replication and had undetectable plasma viremia at week 8 postchallenge. The remaining three vaccinees (V1, V2, and V7) and all four unvaccinated macaques (N1, N2, N3, and N4) failed to control viral replication. Of the five controllers, two macaques V3 and V5 (referred to as transient controllers) exhibited viremia reappearance around week 60, but the other three, V4, V6, and V8 (referred to as sustained controllers), maintained viral control (10).

In the present follow-up study, all seven noncontrollers, including three vaccinees and four unvaccinated controls, exhibited persistent viremia and a gradual decline in peripheral $CD4^+$ T-cell counts (Fig. 1). All of them finally developed AIDS and were euthanized at week 42 to 180 postchallenge (Table 1), confirming that failure in control of SIVmac239 replication results in AIDS progression even in Burmese rhesus macaques. In contrast, all three sustained controllers maintained viral control and preserved peripheral $CD4^+$ T cells without disease progression for more than 3 years (Fig. 1).

We then examined SIVmac239-specific neutralizing antibody responses by determining the end point plasma titers for killing 10-$TCID_{50}$ virus replication on MT4 cells (Fig. 2). Our vaccine regimens did not utilize Env as an immunogen, and no neutralizing antibody responses were induced before challenge in any of the vaccinees. Even after challenge, none of the SIVmac239-challenged macaques showed detectable neutralizing antibody responses until 6 months. After that, neutralizing antibody responses became detectable in some of the noncontrollers. In contrast, no or little neutralizing antibody

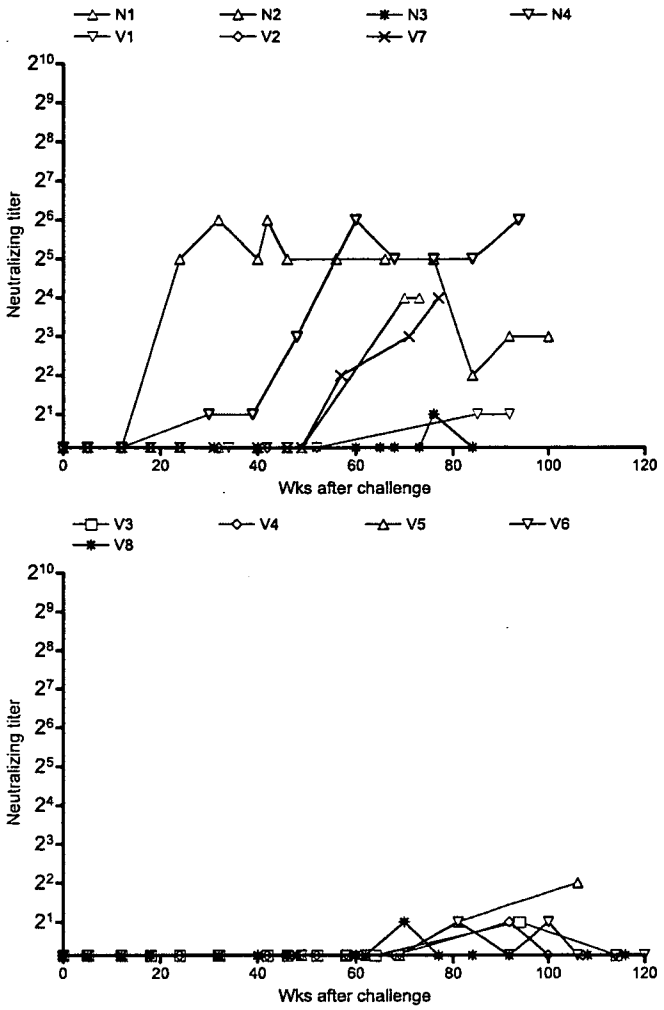

FIG. 2. SIVmac239-specific neutralizing antibody levels in plasma. Plasma titers for killing 10-$TCID_{50}$ SIVmac239 replication in the noncontrollers (top panel), including unvaccinated control animals, and in the controllers (bottom panel) are shown.

responses were induced in the controllers, even in the chronic phase.

Shift of antigens targeted by CTLs during the period of viral control. CTLs from all five controllers selected Gag CTL escape mutations soon after infection, indicating that vaccine-induced Gag-specific CTL responses were crucial for viral control in the early phase of SIV infection (17). In one sustained controller, macaque V4, possessing major histocompatibility complex class I haplotype *90-120-Ia*, $Gag_{206-216}$ (IINEEAAD WDL) epitope-specific CTLs and $Gag_{241-249}$ (SSVDEQIQW) epitope-specific CTL responses likely played a central role in control of viral replication in the chronic phase (10). We also analyzed virus-specific CTL responses in the remaining two sustained controllers, V6 and V8, to determine if vaccine-induced Gag-specific CTL responses played a role in control of viral replication in the chronic phase.

We measured Gag-specific and SIV-specific CTL frequencies in macaques V6 and V8 (Fig. 3). In both macaques, Gag-specific CTL frequencies were high around 2 months postchallenge but then decreased to below detection levels around 1 year postchallenge. In contrast, SIV-specific CTL responses against epitopes in other SIV proteins were still detectable 3 years postchallenge. These results suggest that the vaccine-induced Gag-specific CTL responses were diminished soon after challenge and that there was then a predominance of CTLs specific for SIV-derived antigens other than Gag in the chronic phase in both of the sustained controllers, V6 and V8.

Viremia reappearance by $CD8^+$ cell depletion in the sustained controllers. In the sustained controllers, V6 and V8, vaccine-induced Gag-specific CTLs involved in viremia control in the early phase became undetectable after approximately 6 months. CTLs specific for SIV-derived antigens other than Gag (referred to as SIV non-Gag-specific CTLs) were elicited or expanded after challenge, and these became predominant in the chronic phase. We then performed $CD8^+$ cell depletion experiments to examine if these SIV non-Gag-specific CTL responses played a role in the maintenance of viremia control in the chronic phase. Administration of the monoclonal anti-CD8 antibody, cM-T807, to macaques V6 and V8 at week 156 postchallenge resulted in transient depletion of peripheral $CD8^+$ T lymphocytes (Fig. 4A). In both macaques, plasma viremia reemerged in 1 or 2 weeks after the initial anti-CD8 antibody treatment and disappeared simultaneously with recovery of peripheral $CD8^+$ T lymphocytes in both of them (Fig. 4B). These results support the notion that, in the sustained controllers V6 and V8, these SIV non-Gag-specific CTL responses, rather than vaccine-induced Gag-specific CTL, played a crucial role in the control of SIV replication in the chronic phase. Analysis of the returning wave of virus-specific CTL responses revealed a predominance of SIV non-Gag-specific CTLs (Fig. 4C).

We also administered the anti-CD8 antibody to macaque V5, a transient controller, at week 118. In this macaque, accumulation of multiple Gag CTL escape mutations resulted in reappearance of plasma viremia around week 60. Transient $CD8^+$ cell depletion by the anti-CD8 antibody treatment resulted in a 1-log increase in plasma viral loads (Fig. 1), suggesting that CTLs still exerted pressure on the replication of the escaped viruses at week 118 in this animal.

Long-term central memory $CD4^+$ T-cell preservation in the sustained controllers. It has recently been suggested that vaccine-based transient control of viral replication can ameliorate central memory $CD4^+$ T-cell loss in the early phase of SIV infections. However, it is unclear if CTL-based sustained control of viral replication can contribute to memory $CD4^+$ T-cell preservation in the chronic phase. We, therefore, compared peripheral memory $CD4^+$ T-cell counts at several time points, prechallenge and around weeks 2, 12, 70, and 120 postchallenge, in the noncontrollers and the controllers (Fig. 5). All the noncontrollers showed significant but partial recovery of peripheral memory $CD4^+$ T-cell counts around week 12 after transient loss during the acute phase. However, memory $CD4^+$ T-cell counts, especially central memory $CD4^+$ T-cell counts at week 12, were lower than prechallenge levels in the noncontrollers. By contrast, such a reduction was not observed in the controllers, suggesting protection from acute memory $CD4^+$ T-cell depletion.

A continuous reduction in memory $CD4^+$ T-cell counts was observed in the noncontrollers. The controllers, however, showed no such reduction in memory $CD4^+$ T-cell counts out

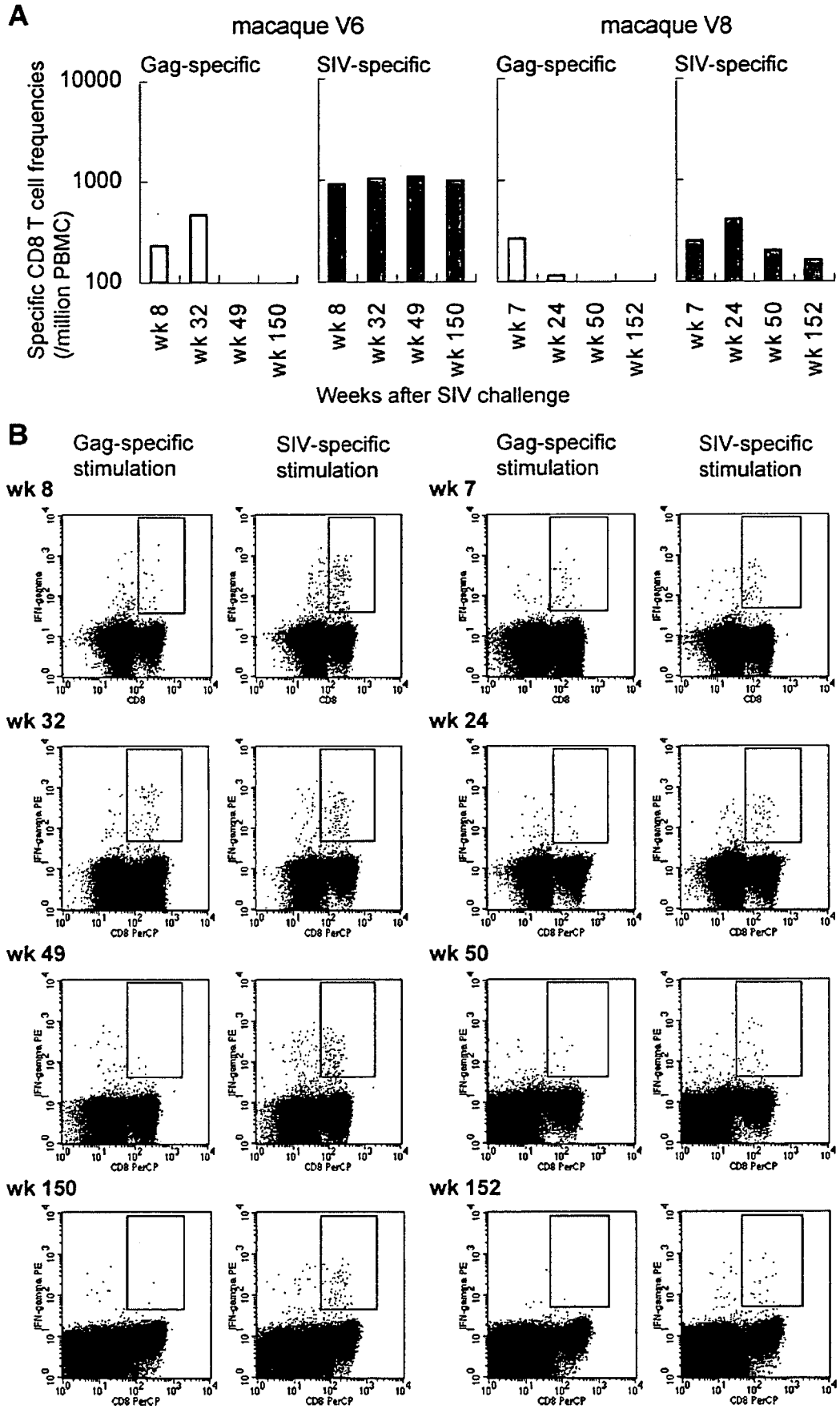

FIG. 3. Virus-specific $CD8^+$ T-cell responses in sustained controllers V6 (left panels) and V8 (right panels). (A) Gag-specific and SIV-specific $CD8^+$ T-cell frequencies in PBMCs. (B) Dot plots gated on $CD3^+$ lymphocytes after Gag-specific or SIV-specific stimulation.

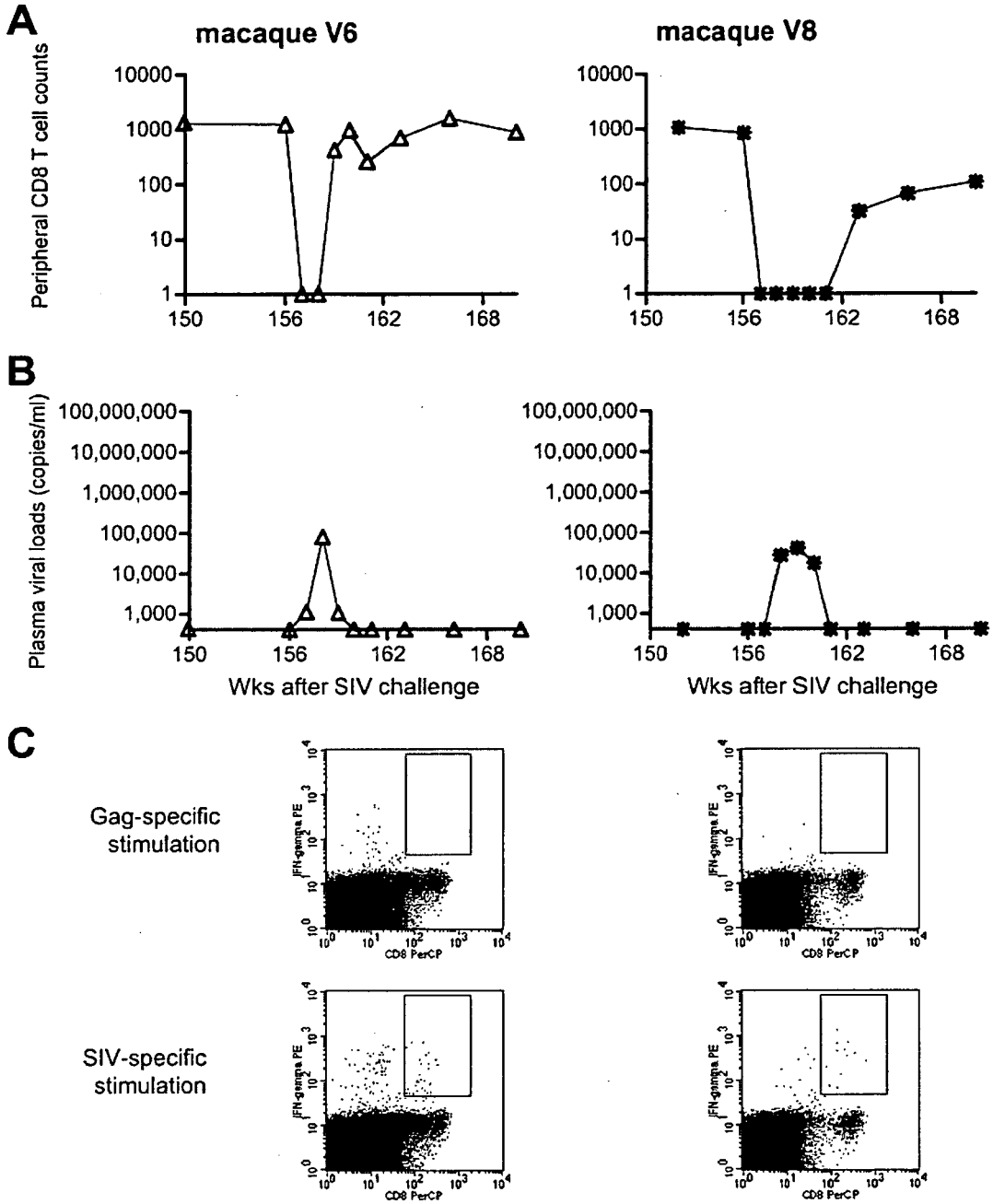

FIG. 4. $CD8^+$ cell depletion experiments starting at week 156 in sustained controllers V6 (left panels) and V8 (right panels). (A) Peripheral $CD8^+$ T-cell counts (per μl). (B) Plasma viral loads (viral RNA copies/ml plasma). (C) Virus-specific CTL responses at week 160 in V6 and at week 166 in V8. Dot plots gated on $CD3^+$ lymphocytes after Gag-specific or SIV-specific stimulation are shown.

to week 70. At approximately week 120, all the sustained controllers still showed preservation of memory and central memory $CD4^+$ T cells. In contrast, both of the transient controllers, V3 and V5, experienced a reduction in central memory $CD4^+$ T-cell counts, although reduction in memory $CD4^+$ T-cell counts was observed in only one of them. These results suggest that CTL-based vaccines that control viral replication can also preserve central memory $CD4^+$ T cells even in the chronic phase. Finally, statistical analysis revealed that there was no significant reduction in central memory $CD4^+$ T cells during the period between weeks 12 and 70 in the controllers (Fig. 6). Thus, CTL vaccine-based, sustained viral control can result in preservation of central memory $CD4^+$ T cells in both the chronic phase as well as the acute phase.

DISCUSSION

Here we followed three Burmese rhesus macaques that maintained CTL vaccine-based control of SIVmac239 replication without disease progression for more than 3 years. The

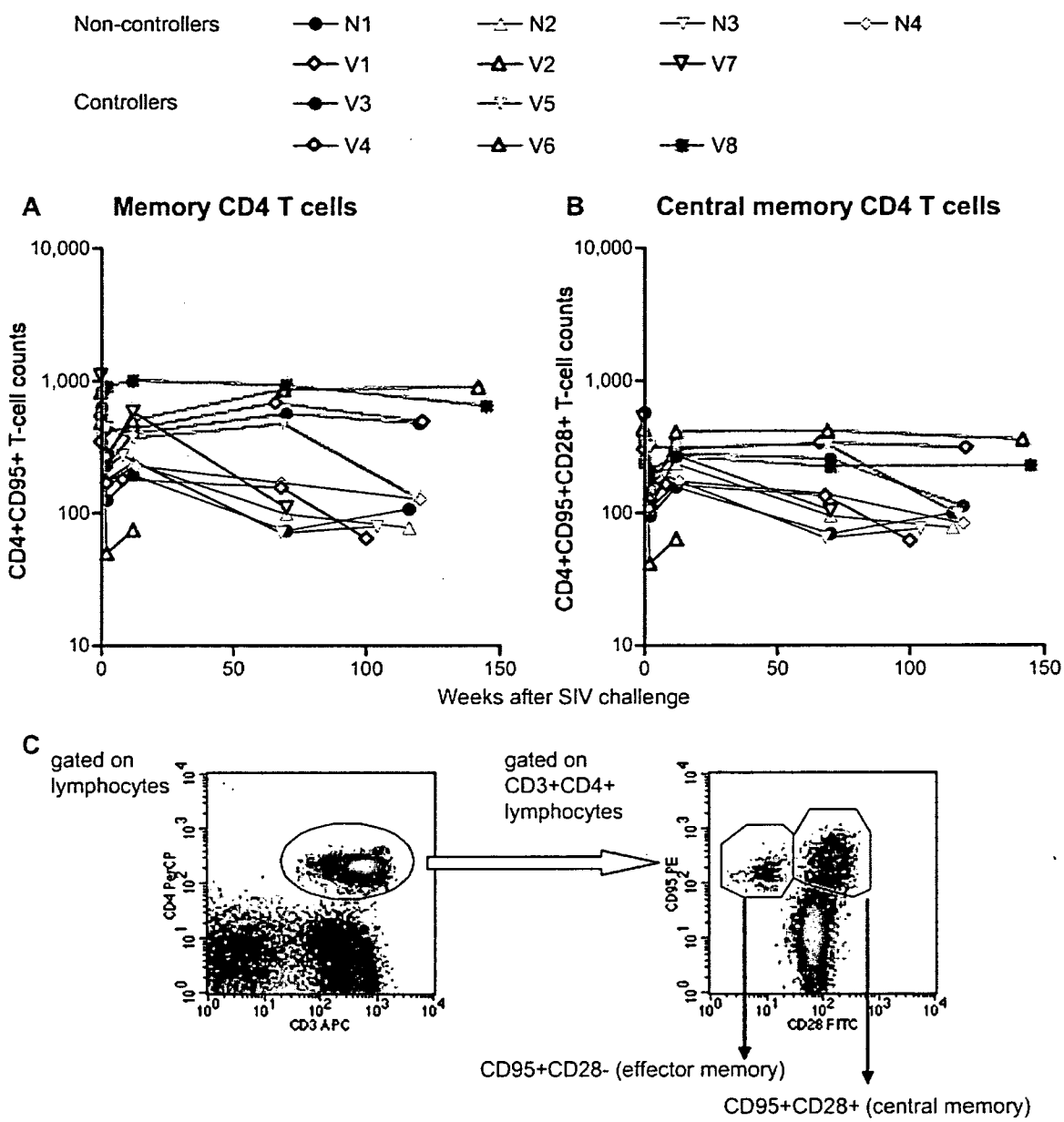

FIG. 5. Changes in peripheral memory $CD4^+$ T-cell counts. Noncontrollers are indicated in black or blue, and controllers are indicated in red. (A) Peripheral memory $CD4^+$ ($CD4^+$ $CD95^+$) T-cell counts (per μl). (B) Peripheral central memory $CD4^+$ ($CD4^+$ $CD95^+$ $CD28^+$) T-cell counts (per μl). (C) Representative density plots (macaque V4 prechallenge) for determining peripheral memory $CD4^+$ T-cell percentages. The left panel is a density plot gated on lymphocytes, and in this plot, $CD3^+$ $CD4^+$ lymphocytes are gated for the right panel of the density plot. In the right panel, we determined the percentages of central memory ($CD95^+$ $CD28^+$) $CD4^+$ T cells and memory ($CD95^+$ $CD28^+$ plus $CD95^+$ $CD28^-$) $CD4^+$ T cells.

set-point plasma viral loads in SIVmac239-infected Burmese rhesus macaques may be lower than those usually observed in SIVmac239-infected Indian rhesus but are higher than those typically observed in untreated humans infected with HIV-1. All four of the naive control animals along with three vaccinees failed to control viremia after SIVmac239 challenge. They also experienced peripheral $CD4^+$ T-cell loss and developed AIDS in 3 years, indicating that this model of SIVmac239 infection in Burmese rhesus macaques is adequate for evaluation of vaccine efficacies. Our finding of long-term control of viral replication and $CD4^+$ T-cell preservation in three vaccinees in this AIDS model underlines the potential of a prophylactic CTL-based vaccine for AIDS prevention.

Our previous study revealed rapid selection of Gag CTL escape mutations in all the controllers, indicating that vaccine-induced Gag-specific CTL responses played an important role in viral control in the early phase of SIV infection (17). In the chronic phase, neutralizing antibody induction was still inefficient, and our results suggest long-term CTL-based viral containment. Indeed, the vaccine-induced Gag-specific CTL responses have been shown to play a crucial role in viral control even in the chronic phase in one (V4) of three sustained